Determining Nipple Position and Smallest Resolvable Volume for Evaluating Breast Reconstruction Surgery

by

Zhale Nowroozilarki

A thesis submitted to the Department of Engineering Technology,

College of Technology

in partial fulfillment of the requirements for the degree of

Master of Science
in Engineering Technology

Chair of Committee: Dr. Fatima A. Merchant, Associate Professor, University of Houston

Committee Member: Dr. George Zouridakis, Professor, University of Houston

Committee Member: Dr. Luca Pollonini, Assistant Professor, University of Houston

University of Houston
July 2020

ACKNOWLEDGMENTS

First of all, I would like to express my deepest appreciation to my advisor, Dr. Fatima A. Merchant, for all of her help and support throughout my graduate years at University of Houston. Dr. Merchant not only has helped me to be a better researcher, but also her dedication to research and teaching has been a source of inspiration for me. Working in her lab was one of the best things that have ever happened in my life which changed my path forever. I would also like to thank Dr. Zouridakis and Dr. Pollonini for serving in my thesis committee and for all of the beneficial tools and knowledge I learned throughout their courses at University of Houston which helped me in completing this degree. Furthermore, I had the pleasure of working with Dr. Greg Reece, Dr. Mia Markey and Dr. Summer Hanson in the ESP Group at MD Anderson Cancer Center which provided me with a priceless set of experience. Also, I would like to appreciate the help of Mary Catherine Bordes and Liu Jun in conducting this research. I would also like to thank my friends and colleagues in the Computational Biology and Medicine Lab, Urmila Sampathkumar, Audrey Cheong and Thao Bui for their help along the way. Also, I would like to thank my fiancé for all of his tremendous support over these years in the United States. I cannot forget to thank my beloved sisters who were always my source of energy to endure all the difficulties of being this far away from my family. Lastly, I would like to thank my parents who have always supported me. They were always my source of motivation. None of these would have been possible without them, their insights and their encouragement.

ABSTRACT

Breast cancer is one of the most widespread cancers among women globally. Because of recent improvements in cancer treatment and increase in survival rate, more women are living with the consequences of breast removal surgery, known as mastectomy. In order to improve the quality of life, physical and psychological well-being after the cancer treatment process, many women decide to have reconstruction surgery. Metrics of breast aesthetics such as position and volume symmetry are often used for outcome assessment following reconstructive surgery. In order to achieve breast symmetry, many measurements which are difficult for human eyes to precisely estimate need to be done. The first aim of this study is to use a data-driven approach to help surgeons annotate the nipple position on reconstructed breast mounds. A graphical user interface was developed to enable computations of nipple localization and symmetry measurements on 3D surface images of pre- and post-operative patients, and a linear regression model incorporating breast aesthetic measures was developed to provide personalized estimate of nipple localization. Secondly, the smallest measurable volume using 3D imaging was analyzed to quantify the resolution of the 3D imaging system. The computational tools and models developed in this study will assist surgeons with surgical planning and outcome assessment and provide a framework for visualization to support physician-patient communication during clinical consultations. This research aims to benefit breast cancer survivors as well as their care givers.

TABLE OF CONTENTS

LIST OF TABLES

LIST OF FIGURES

CHAPTER 1 INTRODUCTION

1.1 Motivation

Breast cancer is one of the most widespread cancers among women in the United States with more than 40,000 deaths and about 276,480 new cancer diagnosis as of 2020. It is also recognized as the most frequently diagnosed cancer in female patients worldwide [1]. One in 8 women in the United States will develop breast cancer over the course of her lifetime. The overall death rate from breast cancer decreased by 1.3% per year from 2013 to 2017. These decreases are thought to be the result of treatment advances and earlier detection through screening [2]. The survival rate is now close to 90% [3] with a majority of the survivors having undergone breast removal surgery also known as mastectomy. Despite the benefits of mastectomy for cancer treatment and the psychological advantage of mitigating the worry about cancer recurrence [4], several women suffer from psychosocial distress related to feminine identity and body image. Breast reconstruction surgery presents an important component of breast cancer treatment following mastectomy, as it has been shown to improve psychological wellbeing, body image and quality of life [5, 6]. There are several factors which play a key role in the outcome of the reconstruction surgeries such as age, body shape, smoking history, previous breast surgeries, medical history, health of the reconstructed tissue, and body weight [7]. There are two main approaches for the reconstruction surgeries: 1) autologous or “flap” reconstruction where tissue is transplanted from another part of the body (e.g., the belly, back, or buttocks) and 2) implant-based reconstruction wherein silicone or saline-filled implants are utilized.

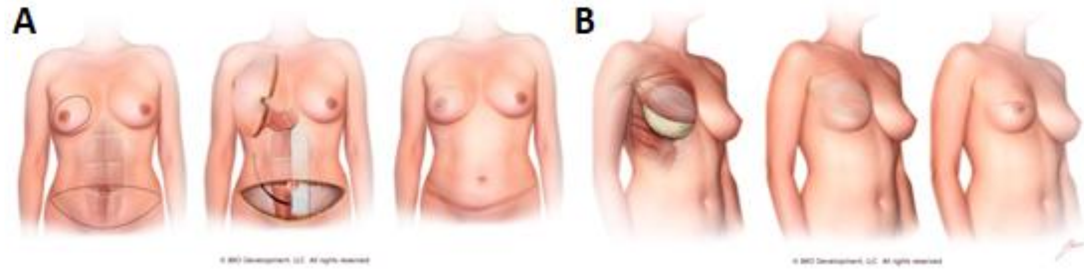

Figure 1.1: Schematic of types of breast reconstruction. (A) Autologous reconstruction [8] and (B) Implant based reconstruction [9].

Furthermore, aesthetic surgeries like breast augmentation and reduction are also common. In most clinics, outcome assessment of breast aesthetics following surgery has been based on surgeon's visual estimation and/or measurements obtained from direct anthropometry or clinical photographs. Outcome assessment for breast surgery has largely relied on qualitative physician-reported [10] or patient-reported measures [11]. Earlier studies involve physicians evaluating breast aesthetics subjectively without the use of imaging tools. Recently, objective measurements have been proposed for clinical assessment using two-dimensional (2D) photographs and three-dimensional (3D) imaging [12]. With the advent of 3D imaging technology, objective measurements, such as contour, surface area, shape, size, and volume are now possible, which were not feasible from 2D photographs. More recent studies have demonstrated the usefulness of three-dimensional scanning and explored the ease of its use and efficiency [13]. Besides breast surgery, 3D imaging has also been widely used to measure some metrics, that improve the quality of care in clinics such as in dental medicine. 3D imaging has been used to simulate treatment planning to maintain patient satisfaction, and as an effective demonstration tool to the patient [14]. In addition, 3D imaging has been used to monitor wound healing status quantitively. For instance, using a mobile application, researchers were able to accurately measure wound area and volume in order to track the status of the wound-healing [15]. Another application of 3D imaging in clinical assessments is to address facial surgery. For example, preoperational planning in cleft orthognathic surgery [16].

In breast surgery, several studies have measured breast symmetry based on anthropometric breast values by recording the linear distance between fiducial points (sternal notch, nipple, midline, and inframammary fold) [17, 18, 19] as well as measuring breast volume [20, 21]. 3D imaging has also shown to offer advantages compared to 2D imaging for objective measurements of breast shape. Cheong et al., quantitatively computed breast ptosis grade (sagginess) using 3D surface images and showed an improvement in accuracy of ~13% compared to conventional 2D methods [22]. Consequently, having a well-developed software or computer application to accurately provide us with objective metrics will result in higher accuracy and more personalized quality of care which can improve patient satisfaction and their quality of life following the clinical operations.

Surgeon's experience and their understanding of the patient's needs and preferences, both play an important role in the outcome of reconstruction surgeries. Thus, there is also a need to objectively define breast aesthetics with the goal of improving patient-physician communication. This would not only allow the physician to communicate expected outcomes but also elicit patient preferences related to their desired breast appearance. Image analysis techniques can bring objectivity to the process, thereby facilitating physician-patient communication and shared decision-making related to treatment choices for breast surgery.

An important determinant of breast aesthetics is bilateral symmetry. Breast symmetry can be assessed by (1) breast position on the torso, which is measured by horizontal or vertical distance symmetry and (2) breast volume symmetry. For example, breast position symmetry can be measured using the ratio of vertical distance between the lowest visible point and sternal notch for the left and right breasts, which represents the vertical extent of the breasts, or the ratio of the horizontal distance from the midline for the left and right breasts, which represents the horizontal extent of breasts. The range of these measurements can vary from 0 to 1. As each of these two ratios approach 1, the corresponding symmetry improves [23].

Volume symmetry of the breasts can be determined by accurately measuring the volume across right and left breast and comparing them. In other words, the ratio of the volume between left and right breast can be used as a metric to evaluate volume symmetry. The ratio of 1 indicates perfect symmetry, while a lower ratio indicates asymmetry in the breasts [24]. While, having symmetrical volume is a key factor in ensuring breast symmetry, it must be accurately measured using computer applications as the exact breast volume cannot be determined by the humans. This is because of very diverse range of breast shapes among women, different types of breast tissues and different postures [25]. Also, artifacts introduced by breathing during image acquisition can result in inaccurate measurements of breast shape and volume. Similarly, difficulty in obtaining a very accurate breast boundary especially in bigger breasts with higher ptosis rates may result in loss of precision for measurements of breast volume. Inconsistencies in volume measurement and lack of appropriate standardization protocols can influence applications that utilize quantitative measurements. For example, changes in breast volume need to be quantified to maintain breast symmetry and any inconsistencies may impede the surgeon's ability to formalize pre-operative plans. In order to achieve optimal symmetry and satisfactory outcome, an understanding of the capabilities and limitations of breast volume measurement is essential in preoperative planning as well as postoperative assessments for both aesthetic and reconstructive surgery. Thus, there is a need for not only having validated algorithms for accurate measurements of breast volume, but to also understand the ability of the technology to resolve and detect volume changes.

Another factor with critical importance in breast reconstruction surgery is the process of nipple reconstruction. Mastectomy surgery typically involves loss of the nipple, which later has to be reconstructed when the breast is rebuild during reconstruction. As a result, the surgeon needs to accurately determine the position of the nipple to maintain the breast aesthetic and patient satisfaction after the reconstruction surgery. Currently, this process is subjective. There is critical need to develop an application to better estimate the position of the nipple on reconstructed breasts for patients whose nipples were removed in their treatment process.

1.2 Objective

The aim of breast reconstruction surgeries is to restore breasts following cancer treatment, thereby improving the quality of life and mitigating body image concerns in patients. There are some factors that help the surgeon in terms of evaluating the result of surgery, however, the factors which will affect patients' satisfaction may differ for each individual [26]. Therefore, it is essential to come up with quantitative criteria to evaluate breast appearance which are also conducive to patient's preferences related to their appearance and consequently impact patient's satisfaction.

The overall goal of this study is to develop tools to enable objective assessment of breast appearance and perform data analytics to provide physicians with normative data on breast shape. The specific objectives of this study are:

1. Quantify the nipple position in natural (pre-operative) breasts in the sample population.
2. Use a data-driven approach to estimate the position of the nipple in post-operative breasts following reconstruction surgery.
3. Develop a phantom to better simulate different breast sizes to assess the accuracy of the equipment and methods in the analysis.
4. Compare 3D surface images taken by a cost-effective portable hand-held scanner versus expensive stereophotogrammetry systems.
5. Investigate the minimum volume measurable by 3D imaging for evaluating volume changes.

CHAPTER 2 RELATED WORK

2.1 Breast Reconstruction

Recent improvement in the quality of care has increased the survival rate in breast cancer patients, and current emphasis is to ensure their physical and psychological well-being after the cancer treatment. In this regard, breast reconstruction surgery has had a significant impact towards improving survivors' psychosocial issues such as anxiety, depression, body image, sexuality and self-esteem [27]. Furthermore, having reconstruction surgeries following mastectomy assist women in mollifying some emotional effects that they have faced from the diagnosis process to the treatment [28]. Patients undergoing immediate reconstruction also have shown better social well-being in comparison to those patients who received delayed reconstruction [29].

The overall goal of breast reconstruction is to restore one or both breasts that were removed during cancer treatment, to near normal shape, appearance, symmetry and size. The other aim of breast reconstruction is to improve the cancer survivor's psychosocial adjustment via improvements in their feminine identity [30]. In order to achieve this goal, the aesthetic aspect of the reconstruction surgery and the improvements of breast appearance are important.

2.2 Breast Aesthetics

Bilateral breast symmetry is a physical trait that is considered aesthetically pleasing and an important objective of breast surgery, be it augmentation, reduction, or reconstruction. Given the psychosocial benefits and impact on physical well-being, it is beyond doubt that maintaining the symmetrical, aesthetical and sexual features of the breasts are among the most fundamental goals in the plastic surgery. Breast aesthetics, however, do not have any universal definition, because the perception of beauty is individualistic, and known to vary with gender, age, and cultural factors 31. Moreover, breast aesthetics also alter with age, weight gain or loss, smoking history, pregnancy and lactation, and bra use [31]. Thus, there is no universal agreement on the appearance of an "ideal" breast, nor any consensus on which attributes of breast shape define attractive breasts. Every woman has her unique body and breast shape. Furthermore, perception of beauty is constantly evolving our time and across cultures. Anthropologists, artists and breast surgeons have long recognized the utility of objective measures such as position, size and their proportions in attractiveness, thus proper measurements and harmonic anthropometric proportions [32] are typically used to assess appearance. For example, in one study, the authors investigated western paintings from mid-nineteenth century to late twentieth century and suggested metrics to define breast aesthetics. They reported that the bilateral distance from the nipple to the sternal notch, and nipple to the midclavicular point was similar, and they were 0.46 of the distance from the sternal notch to the umbilicus. Also, the shape of the projection of the breast was almost an isosceles triangle and the altitude of the triangle was at a proportion of 0.45 with respect to the length of the base of the triangle, and 0.16 of the distance from the sternal notch to the umbilicus [33].

Breast size is another measure that is often reported when assessing breast aesthetics. However, studies have indicated that is not the absolute size, but rather key ratios that influence breast shape and body proportions. Also, breast shape rather than only the volume is critical when estimating breast aesthetics [34]. Studies have examined the correlation between breast size and body size in terms of attractiveness. In a study, 958 participants rated attractiveness of breasts using synthetic images. Fifteen different frontal views in 3 different body sizes and 5 different breast sizes were used as shown in Figure 2.1. The authors of this study reported that breast size obtained the highest rate of attractiveness, but the proportion of the breast size with respect to the body size was also a consideration when rating attractiveness. That is the rating of attractiveness was also highly correlated to shapeliness, i.e. being well-proportioned. This result suggests that the plastic surgeon doing the reconstruction surgeries should not only consider the breast size, but also take the shape of the body into account [35]. Another study in which 128 participants ranked five different breast sizes, showed that the medium to large breasts were ranked to be more attractive [36, 37].

Furthermore, another factor that is important but often overlooked is the bony skeleton and footprint [38]. The footprint is the shape of the outline of the breast as it is positioned on the chest wall and the contour of that interface [39].

Similarly, breast ptosis (sagging) is another metric that is used to assess attractiveness of the breast. In one study, 57 women and 50 men were shown two different ptosis grades using sketches of breasts and were asked to rate the attractiveness of the breasts shown. The result of their study showed that the rating for attractiveness decreased as the breasts were more ptotic. The authors suggest that high ptosis grades often indicate older breasts, while having a lower ptosis grade is an indication of younger age with higher fertility rate and sexual attractiveness [40].

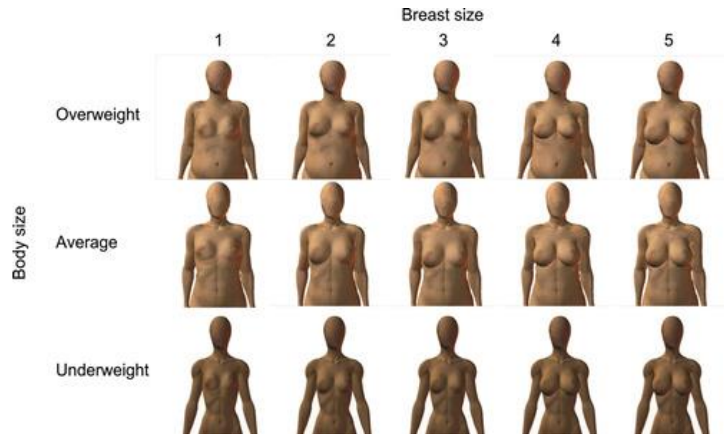

Figure 2.1: Synthetic images used in a study [35] to assess breast attractiveness.

2.3 Ideal Nipple Position

The nipple-areola complex is the focal point of female breasts from a functional (lactation), sexual and aesthetic perspective. Therefore, many patients consider its reconstruction as an important complement to breast reconstruction. Importantly, studies have shown that patients who choose nipple reconstruction surgery report improved psychosocial and sexual well-being [41] and are relatively more satisfied with their breast reconstruction surgery, then women who do not opt for nipple reconstruction [42].

However, estimating the appropriate position of the nipple on the reconstructed breast mound is non-trivial. To date, objective information on nipple position on the breast mound is sparse. Few studies have been conducted with the aim of finding the best possible position for the nipple on the breast mound. For example, in a randomized cross-sectional questionnaire study, 1000 men and 1000 women aged between 16 and 74 years were asked to complete a questionnaire and provide their ranking preference for different nipple positions which were proposed by the authors [43]. The authors used

12 different frontal views as well as 5 profile images to show the volunteers the different ratios they used for the position of the nipple. The ratio of the distance between the lateral point and the nipple and the distance between nipple and midpoint indicates the X-ratio. Similarly, the ratio of the distance between the transition point to the nipple and the distance between the nipple to the inframammary point indicates the Y-ratio. Figure 2.2 shows the visual illustration of the 50:50 X-ratio and 50:50 Y-ratio. Each of the 12 frontal images had a unique combination of X-ratio and Y-ratio. Also, the 5 profile images depicted different ratios among proposed Y-ratios. Figure 2.3 presents the proposed model images from the study. In another study, authors tried to examine an intuitive approach, wherein they deliberately removed nipples from images of 10 young men, and then asked participants images to mark the nipple positions on the images. Resident and consultant plastic surgeons were asked to draw the nipples on the frontal image. The manually annotated positions were then compared to the actual nipple position [44]. They found out a significant deviation in the marked positions among the participants. Furthermore, the participants annotated the horizontal height of the nipple more accurately than the vertical position. They also concluded that a combination of different factors such as the intuition form multiple plastic surgeons, patient needs, and practical metric method will better determine the position of areola complex-nipple area. Furthermore, in order to come up with the natural nipple-areola-breast proportion and to also provide a general guideline for the surgeons to have the optimal surgery outcome, in another study the anatomic size of the nipple, areola and breast was measured in 37 women aged 20 to 64 years, and their proportions were calculated. The areola-breast and nipple-areola proportions were found out to be 1:3.4 and 1:3, respectively [45]. In

a similar study, authors investigated aesthetic characteristic of non-operated breast. They asked 3 observers to measure base width, nipple diameter and areolar diameter of 58 model images independently. Next, the ratios of the areolar diameter to the base width and the nipple diameter were calculated. They concluded that the average areolar diameter to base width was 0.29 (SD = 0.05) and the average nipple to areolar diameter was 0.29 (SD = 0.06) [46]. In another study, the authors mentioned that ideal breast shape follows a ratio called golden ratio which is among the submammary fold, nipple-areola complex border, and sternal midline. In order to come up with this golden ratio, they defined a V-shaped triangle with the vertex situated at the umbilicus and the other two 2 branches of the isosceles triangle opening at an angle of approximately 60° from the umbilicus point and close to the acromioclavicular articulation. The result of this study was as follows: 83% of the patients received a good score. 7% of the patient had complication in the healing process with minimal scars, 6% of the patients experienced asymmetry in their breasts and finally about 4% of the patients experienced partial nipple necrosis [47]. Although the result of their approach was not 100% as expected, they proposed a new method in evaluating aesthetic breast shape.

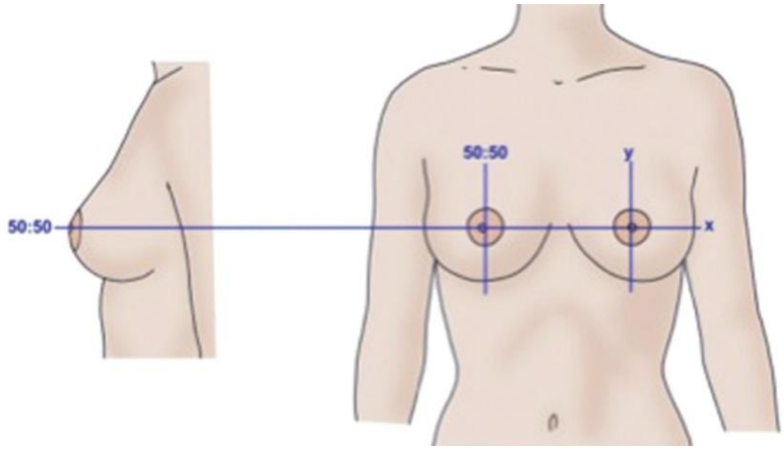

Figure 2.2: An example of nipple-areola complex placement in a 50:50 *X*- and *Y-ratio*. Figure from [43]

Figure 2.3: Twelve frontal images and the 5 profile images, with associated *X*- and *Y-ratio*s. Image from [43]

A limitation of studies that proposed metrics for ideal nipple positions is the lack of diverse datasets representative of breasts of varying size and shape. One of the aims of this study is to develop metrics for nipple position by utilizing a sample population that represents diversity in terms of patient demographics and breast shape. Furthermore, for patients following mastectomy who want to have symmetrical and well-shaped breasts, this study will introduce the required measurements and ratios to help patients in the decision-making process, as well as improve physician-patient communication during clinical consultations.

2.4 Bilateral Symmetry of Breast Position and Breast Volume

There are many factors which have been shown to lead to higher satisfaction after the reconstruction surgery such as symmetry across the left and right breasts, breast size and shape, not having scars and nipple reconstruction [48]. Bilateral breast symmetry is a physical trait that is considered aesthetically pleasing and an important objective of breast surgery, be it augmentation, reduction, or reconstruction [49]. Breast symmetry is typical evaluated in terms of breast position or breast size. For example, in one study [23], vertical extent and horizontal extent symmetry values, which are indicators of breast symmetry across the vertical axis, were calculated from clinical photographs. Moreover, the authors tried to find correlation between these metrics and the patients' dissatisfaction rates by running multiple regression analysis. They found out that vertical extent symmetry, but not horizontal extent symmetry, was associated with body image dissatisfaction.

2.5 Volume Measurement Techniques

Breast volume symmetry is another metric for assessing breast surgery outcome. However, it is difficult to assess volume changes manually due to the very diverse range of breast shapes among women, different types of breast tissues, and different postures [50]. In addition, breathing artifacts may also mitigate the accuracy of measurements of breast shape and volume changes. Similarly, the size of the breast may also impede accurate objective assessment of breast shape. For example, shape and volume assessment is difficult for bigger breasts with higher ptosis rates, due to the challenges associated in delineating the breast boundary or footprint. There is a critical need to improve our knowledge of volume symmetry by providing accurate volume measurement algorithms, while also providing an assessment of the limits of current clinical instruments and algorithms. Accurate breast volume measurement is among those factors which is essential in the preoperative planning as well as the postoperative assessments for both aesthetic and reconstructive surgery in order to achieve the best symmetry and satisfactory outcome. Therefore, having a method/software to accurately measure the volume in daily clinical practice is highly appreciable.

There are different techniques to measure the breast volume such as mammography, anthropometry, thermoplastic casting, the Archimedes procedure, the Grossman-Roudner device, Computed Tomography, ultrasonography and Magnetic Resource Imaging [51 - 55]. While the water displacement approach is inexpensive and straight forward, it is cumbersome and not pragmatic for clinical use due to patient inconvenience and its time-consuming aspect. Also, it is not feasible to use this approach for many patients during postoperative stages. The other method which is considered as a gold standard for volume measurement is using MRI imaging for both diagnosis and assessments [56]. Although, we can obtain a fairly accurate measurement using MRI images, its costs per measurement could be very expensive and the whole procedure could be time consuming as well.

Recently, 3D imaging has gained a lot of attention because of its many advantages. Most importantly, it is a non-invasive procedure which has little to no difficulty for patient. Furthermore, it is very quick, relative to other methods like MRI. Also, the patient can be imaged in standing position which is closer to the natural look of breast. To summarize, 3D stereophotography can be done quicker, it is non-invasive and less expensive, and more convenient when compared to other non-optical methods for 3D imaging.

Breast volume plays a key role in determining breast symmetry and more generally the quality of reconstruction surgery. As a result, we need to be aware of the error range of the equipment or the software that we use for volume measurements to better rely on the provided numbers. For example, in a study, the authors investigated the validation of the Vectra XT 3D imaging system for measuring breast volume and breast volume symmetry following oncological reconstruction. They created some phantom models with volume ranging from 100 and 1000 cc to mimic breasts of different sizes. Furthermore, they asked two observers to measure the volume using the Vectra XT 3D-SI™ system. In addition to the simulated phantoms, they asked observers to measure the breast volume and symmetry in 16 patients who had undergone oncological breast surgery [57]. They reported intra-observer mean coefficients of variation also known as CV factor of 0.58% and 0.49% and inter-observer variation CV factor of 0.11% in phantom measurements between observer one and two respectively. Also, they reported intra-observer variation of 8 and 14% (mean CV) and the mean relative difference of 0.43 mm for average symmetry values in range of 3.5 to 15.5 mm between the observers for the shape symmetry measurements. Furthermore, in another study, the accuracy of three software applications for breast volume calculations from 3D surface images was investigated by comparing against the mastectomy specimen as the gold standard. They proposed an error rate of less than 5% of breast volume as an acceptable range [58].

In order to accurately define the breast volume to ensure highest possible patient satisfaction rate, some minimum criteria need to be taken into account. In one study, the authors used an adapted Delphi method to elicit views of the professional care givers and user representatives. Delphi method is a way to achieve consensus on a specific topic in a group consisting of experts on the topic which being studied. In this method, questionnaires are sent to the panel in multiple rounds and the correct response is obtained through consensus [59]. In this study, the participants were asked to provide their views on the requirements of the 3D imaging system in order to develop consensus on the minimum standards [60]. The result of the Delphi evaluation was then used to develop a low-cost 3D surface imaging system is as follows:

1. Calculate the volume with an accuracy of ±5%
2. Detect a volume difference of 25 cc or over
3. Measure distances with an accuracy of ≤ 5 mm

4. Be able to capture marks placed on the nipple, base width of the breast, lateral edges of the breast, the mid-line of the sternum, inframammary fold, and superior pole of the breast.
5. Cost less than £10,000
6. Fit a space $< 4\ m^2$
7. Produce 3D images that are easily manipulated without much prior experience.

CHAPTER 3 METHODS AND MATERIALS

3.1 Image Acquisition

3D surface images were acquired at the MD Anderson Cancer Center (Houston, TX), using two different devices 3dMDtorso™ system (3dMD® LLC, Atlanta, GA) and Go! Scan3D handheld scanner (Creaform Inc., Canada). Both devices output the 3D shape of the objects by providing the triangular mesh or the point cloud. If the texture image is also available, it can be overlaid on the triangular mesh to provide realistic displays of the imaged object.

(A) (B) (C)

Figure 3.1: Three different displays of a single 3D image obtained using the 3dMDtorso™ system: A) 2D texture overlaid on the 3D surface mesh, B) 3D point cloud, and C) 3D triangular surface mesh.

The 3dMDtorso™ system is equipped with six modular cameras which use stereophotogrammetry to estimate a 3D surface image from pairs of 2D photographs. The overview of this imaging system is shown in the Figure 3.2 [61].

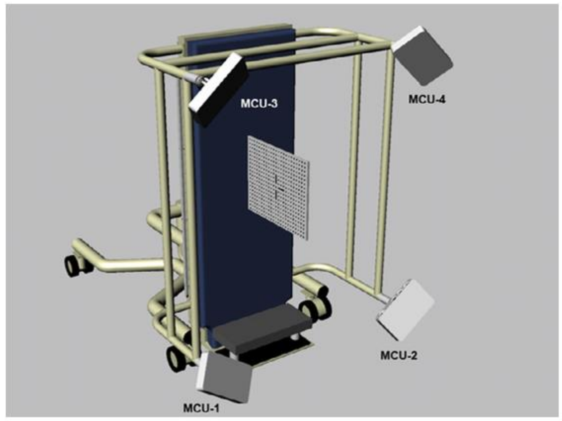

Figure 3.2: Customized 3dMDTorso imaging system at MDACC consisting of four modular camera units [61] .

The second imaging device that was used in this study is Go!Scan 3D portable hand-held scanner. This portable scanner uses structured light 3D scanning technology and is equipped with the VXelements^{TM} software that facilitates scanning. In order to capture the topology of the object, which is being scanned, the device flashes a light with a specific pattern (e.g. similar to a QR code) which is cast on the 3D object. In this regard, the light which is cast on the object deforms based on the formation and the topology of the object. The two cameras of the Go! SCAN 3D hand-held scanner register this deformation and the software is then able to compute the 3D properties of the object. The device model which was used in this study did not capture the texture of the object's surface. But, for device models with the capability to capture the texture, the data is captured as a colored dots cloud which is then used to generate an accurate 3D mesh on which a texture mapping (the color) can be applied [62].

Figure 3.3: Go!Scan^{TM} 3D hand-held scanner

3.2 Volume Measurement Software

In order to measure the volume, we used a customized software called Breast Research (BR) which had been developed and validated by our research team [63]. BR is a java-based software which facilitates interactive visualization of 3D images, annotation of fiducial points, and measurements of Euclidean as well as the contour distance between points, registration and overlay of 3D images, and volume measurements.

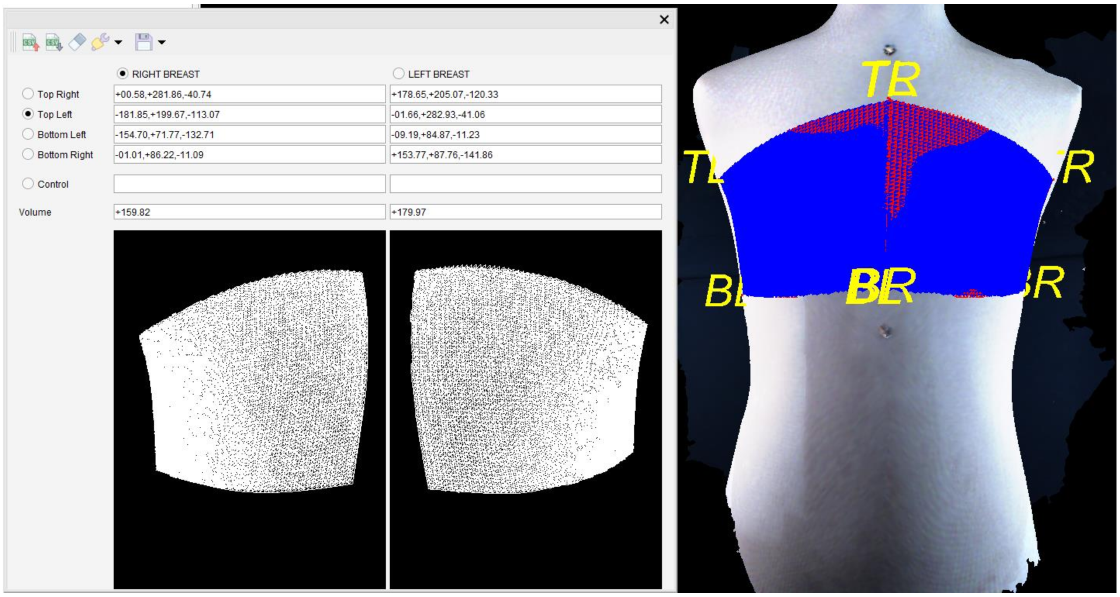

Figure 3.4: Volume measurement in BR software.

3.3 Adjustable Implants

In order to simulate different breast sizes in different orientations, we used saline-filled adjustable volume breast implants, fitted with a fill tube for allowing injection of varying amounts of water to achieve desired size adjustments. Three different sizes of adjustable implants (354-2511: 275–330 cc, 354-2514: 550–660 cc, and 354-2515: 650–780 cc) were donated by Mentor Worldwide LLC, Irvine, CA. The implants were painted with washable paints to minimize reflective glare and 3D surface images were acquired using the 3dMDtorso™ system (3dMD® LLC, Atlanta, GA).

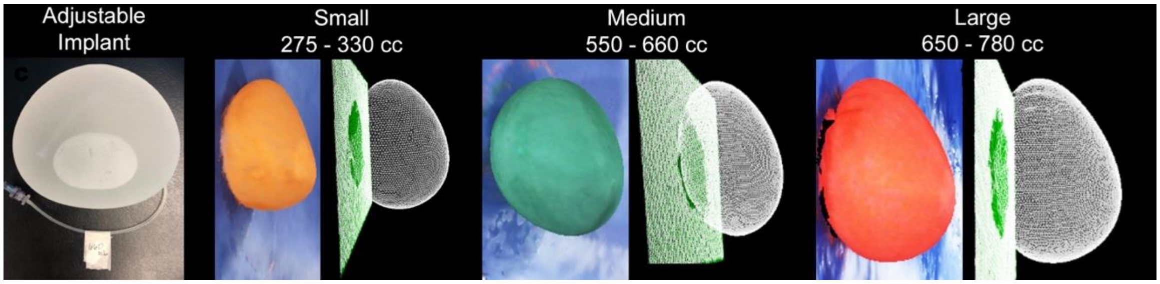

Figure 3.5: Water-filled adjustable implants in three different sizes and their 3D surface mesh images.

3.4 Subject Population

The study sample consisted of adult female patients undergoing treatment at the Center for Reconstructive Surgery at The University of Texas MD Anderson Cancer Center between 2011 and 2014.

Table 3.1: Demographics of the subject population of the training set including 87 patients at pre-operative time point.

Variable	**Statistics**
Age, years	
Mean ± STD	48.6 ± 10.5
Median (range)	47 (28 to 73)
BMI, (body mass index) kg/m^2	
Mean ± STD	26.7 ± 5.1
Median (range)	25.6 (18 to 41)
Variable	**N (%)**
Race	
Caucasian	65 (74.7)
African American	6 (6.9)
Asian	4 (4.6)
Other	4 (4.6)
Not available	8 (9.2)
Ethnicity	
Hispanic	13 (14.9)
Not Hispanic	64 (73.6)
Not Available	10 (11.5)
Pre-operative Chemotherapy	
Yes	34 (39.1)
No	53 (60.9)

Table 3.2: Demographics of the post-operative subject population including 24 patients (39 reconstructed breasts) used for calculating the average X-ratio and Y-ratio

Variable	**Statistics**
Age, years	
Mean ± STD	48.9 ± 8.8
Median (range)	47 (35 to 68)
BMI, (body mass index) kg/m^2	
Mean ± STD	28.1 ± 5
Median (range)	27 (21 to 38)
Variable	**N (%)**
Race	
Caucasian	18 (75)
African American	1 (4.2)
Asian	1 (4.2)
Not Available	4 (16.6)
Ethnicity	
Hispanic	3 (12.5)
Not Hispanic	18 (75)
Not Available	3 (12.5)
Pre-operative Chemotherapy	
Yes	8 (33)
No	16 (66)
Reconstruction Type	
Implant	29 (breasts) (74.3)
Autologous	10 (breasts) (25.7)

Table 3.3: Demographics of the subject population for the validation set including 20 patients at pre-operative time point.

Variable	**Statistics**
Age, years	
Mean ± STD	46.1 ± 10.2
Median (range)	47 (24 to 65)
BMI, (body mass index) kg/m^2	
Mean ± STD	29.1 ± 6.6
Median (range)	27.2 (18.5 to 40)
Variable	**N (%)**
Race	
Caucasian	15 (75)
African American	2 (10)
Not Available	3 (15)
Ethnicity	

Hispanic	4 (20)
Not Hispanic	15 (75)
Not Available	1 (5)
Pre-operative Chemotherapy	
Yes	8 (40)
No	12 (60)

Table 3.4: Demographics of the subject population for the validation set including 24 post-operative patients at 3M time point with tissue expander (TE).

Variable	**Statistics**
Age, years	
Mean ± STD	43.4 ± 10.3
Median (range)	41.5 (30 to 68)
BMI, (body mass index) kg/m^2	
Mean ± STD	25.8 ± 4.1
Median (range)	25 (18.1 to 36)
Variable	**N (%)**
Race	
Caucasian	21 (87.5)
American Indian Alaskan	1 (4)
Not Available	2 (8)
Ethnicity	
Hispanic	4 (16.7)
Not Hispanic	17 (70.8)
Not Available	3 (12.5)
Pre-operative Chemotherapy	
Yes	5 (21)
No	19 (79)

Table 3.5: Demographics of the subject population for the validation set including 9 post-operative patients at more than 9M time point with reconstructed breast.

Variable	**Statistics**
Age, years	
Mean ± STD	54.1 ± 8.7
Median (range)	54 (42 to 67)
BMI, (body mass index) kg/m^2	
Mean ± STD	29.4 ± 6.2
Median (range)	26.33 (22.7 to 39.3)
Variable	**N (%)**

Race	
Caucasian	7 (77.8)
African American	2 (22.2.)
Ethnicity	
Hispanic	1 (11.1)
Not Hispanic	8 (88.9)
Pre-operative Chemotherapy	
Yes	1 (11.1)
No	8 (88.9)
Reconstruction Type	
Implant	8 (breasts) (72.7)
Native Breast with Revision	3 (breasts) (27.3)

The data in this study come from a prospective Institutional Review Board–approved research project that enrolled patients at various stages of breast reconstruction. Participants provided written informed consent. Images were usually taken in each 3-month (M) period during the time frame of their reconstruction. 3D surface images from 87 patients (174 breasts) at the pre-operative visit and 24 patients (39 breasts) at the post-operative visit used as the training data set. In addition, 20 patients (40 breasts) at the pre-operative visit, 24 patients (48 breasts) at the 3M visit when patients had completed TE (TE) placement (which includes placing a temporary implant to stretch the skin and prepare the skin tissue for reconstruction) and 9 patients (11 breasts) at post-operative visit, i.e. more than 9 Ms of time interval from their baseline visit, were used as the validation data sets. Demographics of the 87 subjects used for training the linear regression analysis, 24 subjects were used to calculate average post-operative X-ratio and Y-ratio, 20 subjects used for pre-operation validation analysis, 24 subjects with TE at 3M time point used for post-operative validation analysis and 9 subjected at more than 9M time point used for post-operative validation analysis are shown in Table 3.1, Table 3.2, Table 3.3, Table 3.4, Table 3.5 respectively.

3.5 Statistical Analysis

For data analysis on estimating the nipple position based on *X*- and *Y-ratio*, descriptive statistics, such as means, standard deviations, median and range were applied to present age, BMI, height, breast volume, nipple *Y-ratio*, nipple *X-ratio*, sternal notch to nipple ratio and lowest visible point to sternal notch (vertical ratio). Frequency counts and percentages were used to present race, ethnicity and ptosis grades. Linear regression models and ANOVA were used to assess the relationship between nipple *Y-ratio* or nipple *X-ratio* and predictive variables. A multiple linear regression model was fitted using stepwise model selection procedure. Residuals were examined to assess model fit. The multiple collinearity was checked with variance inflation factors. Tukey-Kamara method was applied for multiple comparisons. All tests were two-sided. Statistical significance was set at $p<0.05$. All analyses were performed using SAS 9.4 (SAS Institute Inc., Cary, NC, USA).

CHAPTER 4 RESULTS

4.1 Estimation of Nipple Position

In order to quantify the nipple position in breasts, a Graphical User Interface (GUI) was developed to determine the X- and Y-ratios evident in the sample population. To determine characteristics of breast aesthetic that could influence nipple position, the GUI also enabled measurements of distance symmetry.

4.1.1 GUI Development

The GUI was developed using MATLAB® (The Mathworks, Natick, MA), and has multiple features to enable measurements of vertical symmetry using different fiducial points, and support annotation and visualization of different X- and Y-ratios for nipple positioning.

The GUI supports annotation of the following fiducial points of the breast, including sternal notch (SN), lateral point (LP), transition point (TP), inframammary fold point (IMF), medial point (MP), nipple (N) and lowest visible point (LVP). Using the coordinates of the annotated fiducial points, the software computes distances and X- and Y-ratios, and displays the estimated nipple positions for different ratios for user visualization and assessment.

In order to investigate symmetry, two measurements can be obtained from the GUI. First, the Euclidean distance between sternal notch and each nipple, and second the vertical distance between sternal notch and lowest visible point on the breast.

The GUI calculates and displays three previously reported "ideal" nipple positions [44], including the 50:50 X-ratio and 50:50 Y-ratio, 40:60 X-ratio and 40:60

Y-ratio, and 40:60 X-ratio and 50:50 Y-ratio. Additionally, a data-driven estimate of the nipple position computed from images of post-operative patients who had completed their surgery with nipple reconstruction is provided. A screenshot of the GUI is shown in Figure 4.1 and features are listed below:

1. Open 3D surfaces images in the "x3d" format and overlay the texture of the image provided in "png" format.
2. Interactive click-enabled annotation and display of color-coded fiducial points.
3. Interactive click-enabled annotation and display of 4 color-coded index lines that define the bounding rectangle enclosing each breast.
4. Visualization of the X- and Y-axes within the bounding rectangles enclosing each breast.
5. Interactive 360° rotation of displayed images and overlaid annotated points and lines.
6. Interactive zoom-in and zoom-out visualization.
7. Interactive turn-on and turn-off feature to display points and lines and single-click feature for undoing an annotation or clearing all annotations.
8. Calculation and display of the following values: SN-LVP and SN-N distances, and the X-ratio and Y-ratio for each annotated nipple.
9. Display of the color-coded estimated nipple position for the three different ratios (50:50 X-ratio and 50:50 Y-ratio, 40:60 X-ratio and 40:60 Y-ratio, and 40:60 X-ratio and 50:50 Y-ratio), as well as for data-driven estimate of nipple position.
10. Support for saving coordinates of annotated fiducial points and calculated measurements in "csv" format that is compatible for import into data analytics

software, such as Microsoft Excel and the customized BR software developed at UH.

11. Seamless data exchange across the BR software and the GUI.

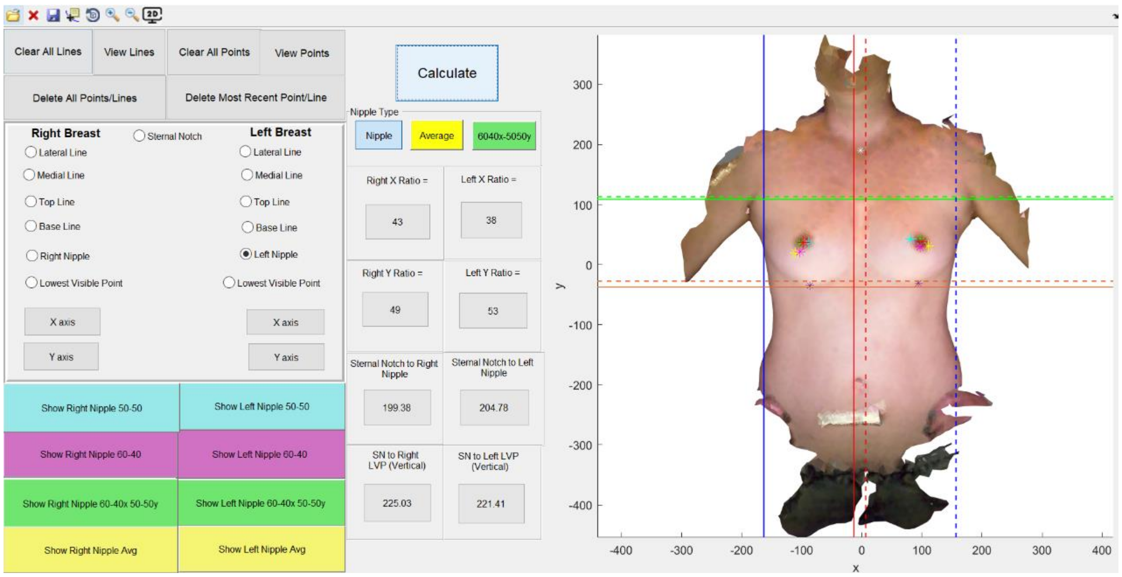

Figure 4.1: Screenshot of the developed graphical user interface.

4.1.2 Nipple Position Analysis in Natural Breasts (Specific Objective 1)

The nipple position was annotated for 174 breasts in 3D surface images using the GUI and the X- and Y-ratios were computed. Additionally, in order to determine the association of nipple position with patient demographics and breast aesthetics, the ptosis grade was recorded for each breast, and breast volume and distance from the sternal notch to the nipple (SN-N) and sternal notch to the lowest visible point (SN-LVP) were computed. The following demographics factors: BMI, age, race and ethnicity, and breast appearance factors: ptosis grade, SN-N distance, SN-LVP and breast volume were analyzed to determine any association with nipple position represented in terms of X-ratio and Y-ratio. Results from univariate analysis of demographic factors and breast aesthetic factors are shown in Figure 4.2 and Figure 4.3, respectively.

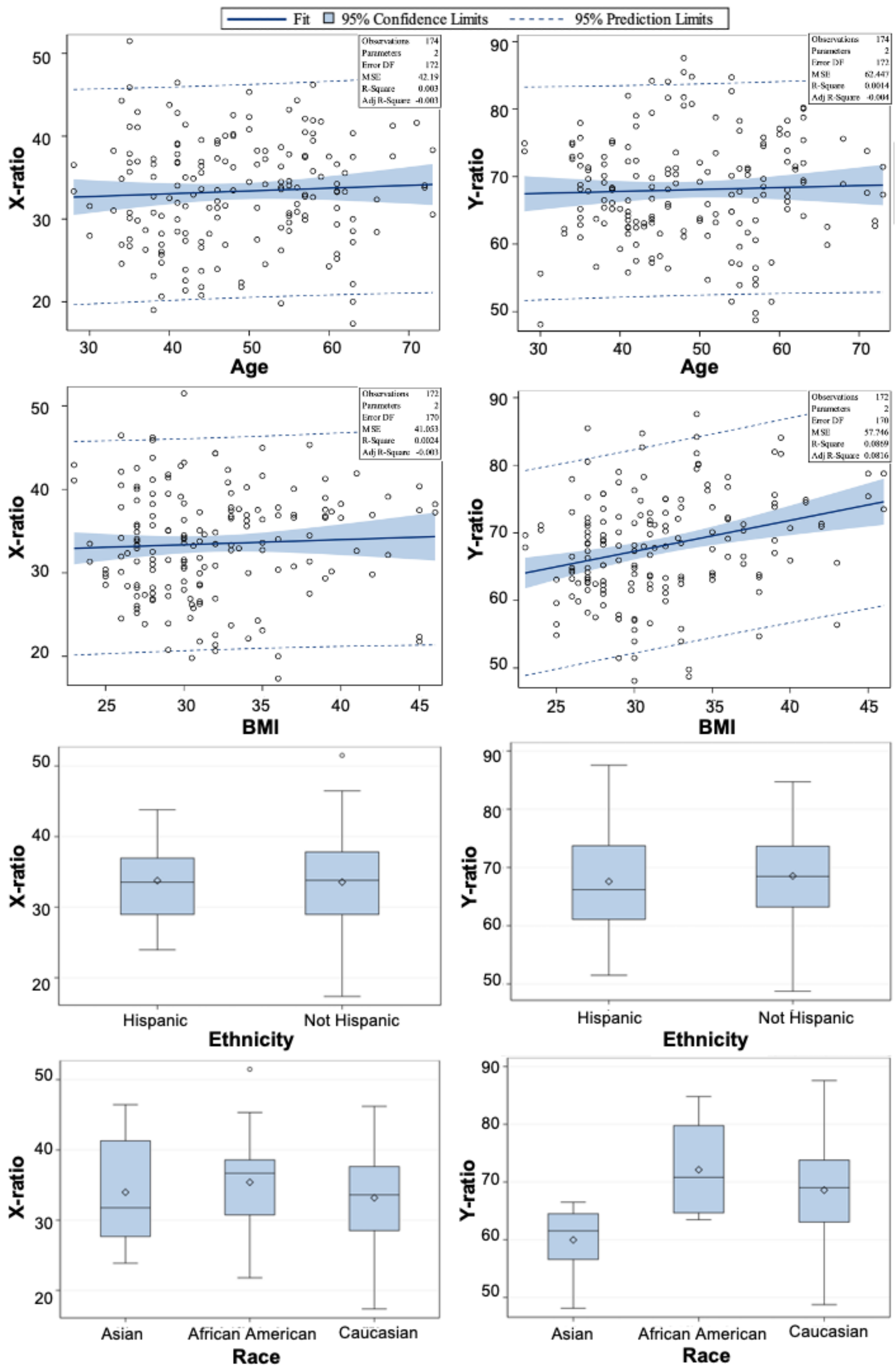

Figure 4.2: Univariate analysis of nipple position X- and Y-ratio with demographic factors.

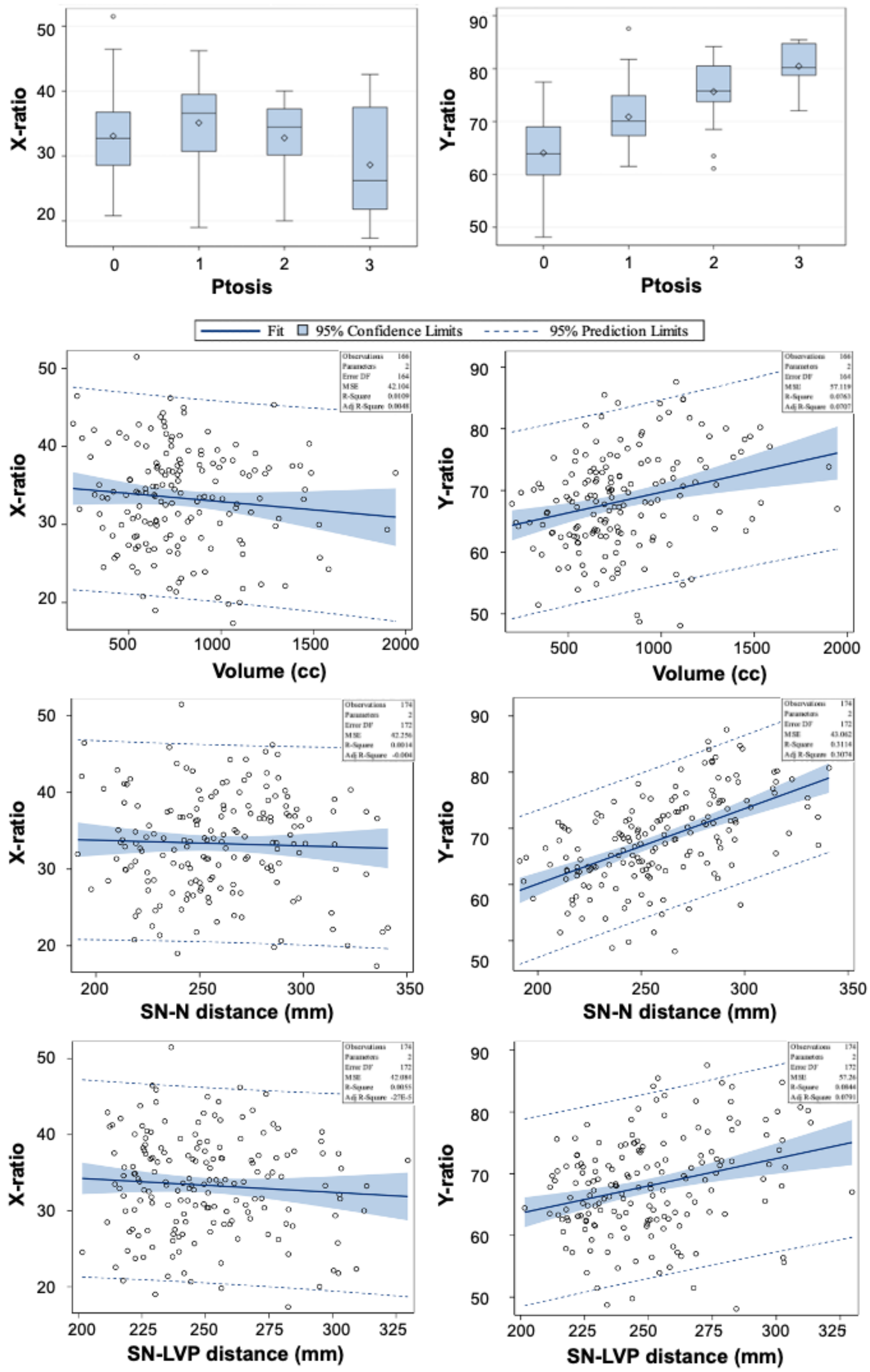

Figure 4.3: Univariate analysis of nipple position X- and Y-ratio with breast aesthetics factors.

Next correlation analysis was performed to determine any associations across the various demographic and breast aesthetic factors as shown in Table 4.1 below.

Table 4.1: Descriptive statistics and correlation among variables.

Variable	N	Mean	Std Dev	Minimum	Maximum
Y-ratio	174	68.0	7.9	48.1	87.6
X-ratio	174	33.3	6.5	17.3	51.5
Age	174	48.6	10.5	28.0	73.0
BMI	172	26.7	5.1	18.0	41.0
Volume	166	794.0	323.4	197.1	1946
SN–N Distance	174	259.2	32.9	191.2	340.8
SN–LVP Distance	174	250.2	25.9	201.5	329.6

Pearson Correlation Coefficients, Prob > \|r\| under H0: Rho=0, Number

	Y-ratio	X-ratio	Age	BMI	Volume	SN–N	SN–LVP
Y-ratio	1.00 174	0.03 0.71 174	0.04 0.62 174	0.30 <.0001 172	0.28 0.0003 166	0.56 <.0001 174	0.29 0.0001 174
X-ratio	0.03 0.71 174	1.00 174	0.05 0.47 174	0.05 0.53 172	-0.10 0.18 166	-0.04 0.62 174	-0.07 0.33 174
Age	0.04 0.61 174	0.05 0.47 174	1.00 174	0.09 0.22 172	0.14 0.07 166	0.21 0.006 174	0.25 0.0007 174
BMI	0.30 <.0001 172	0.05 0.53 172	0.09 0.21 172	1.00 172	0.68 <.0001 164	0.67 <.0001 172	0.41 <.0001 172
Volume	0.28 0.0003 166	-0.10 0.18 166	0.14 0.07 166	0.68 <.0001 164	1.00 166	0.83 <.0001 166	0.71 <.0001 166
SN–N	0.56 <.0001 174	-0.04 0.62 174	0.21 0.006 174	0.67 <.0001 172	0.83 <.0001 166	1.00 174	0.77 <.0001 174
SN–LVP	0.29 0.0001 174	-0.07 0.33 174	0.25 0.0007 174	0.41 <.0001 172	0.71 <.0001 166	0.77 <.0001 174	1.00 174

Correlated variables were identified based on values of Pearson Correlation Coefficients > 0.5 and p-values < 0.05. Multiple linear regression model fitted using stepwise model selection procedure generated a model for Y-ratio as shown in Table 4.2. Ethnicity was not a significant factor for the Y-ratio and race was found to be significant in univariate analysis but not in multivariate model.

Table 4.2: Multivariate linear regression model for Y-ratio

Parameter	Estimate	Std. Error	t Value	Pr > |t|
Intercept	64.7	6.3	10.30	<.0001
Ptosis Grade 0	-12.8	2.5	-5.14	<.0001
Ptosis Grade 1	-7.6	2.3	-3.33	0.0011
Ptosis Grade 2	-3.6	2.4	-1.49	0.1387
Ptosis Grade 3	0.0	.	.	.
SN–N	0.05	0.02	2.63	0.0093

The model shows that ptosis is significantly associated with higher Y-ratio. As shown in Figure 4.4, compared to patients with ptosis grade 0, the patients with ptosis grade 1, 2 and 3 are 5%, 9% and 13% greater on Y-ratio, respectively. Sternal notch to nipple distance is also significantly correlated with Y-ratio, with every sternal notch to nipple increase by one unit, resulting in a Y-ratio increase of 0.05%.

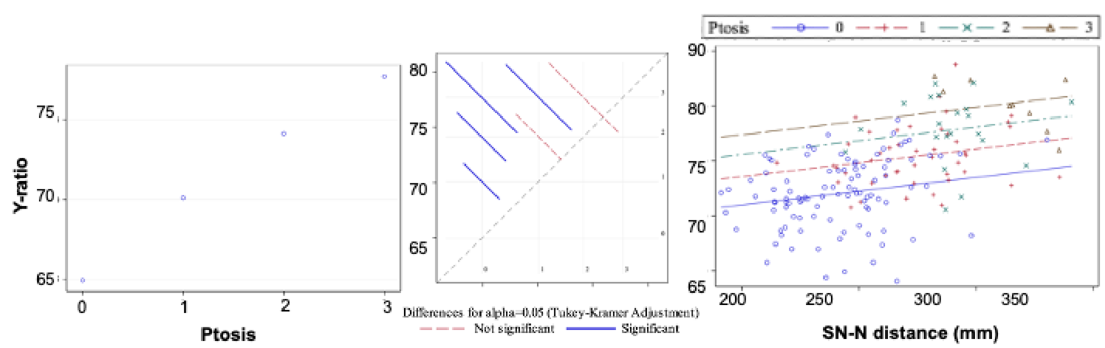

Figure 4.4: Least-square means adjustment for ptosis and Y-ratio and analysis of covariance for SN-N distance and Y-ratio.

There was no clear trend between X-ratio and ptosis, with the lowest X-ratio observed for ptosis grade 3 and the highest X-ratio observed for ptosis grade 1 as shown in Table 4.3. The p-value was 0.03 < 0.05, which suggests significant difference on X-ratio among the four ptosis grades. However, pairwise comparison indicated that significant difference exists only across grades 1 and 3.

Table 4.3: Association between X-ratio and ptosis

Level of Ptosis	N	Nipple X-ratio	
		Mean	Std Dev
0	99	33.0782188	6.04617621
1	45	35.1056601	6.52531445
2	21	32.7798442	6.15329702
3	9	28.6280082	9.43220799

4.1.3 Inter-Observer Variability Analysis

Three observers who were provided with instructions and a demonstration of the GUI, annotated fiducial points and index lines on the training set of 87 pre-operation images. Annotations by the three observers were assessed to determine inter-observer variability. Intraclass Correlation Coefficient (ICC) [64] was used to investigate the inter-observer variability in measuring the SN-N distance, the SN-LVP distance, and the nipple X- and Y-ratios. In this study, ICC values were interpreted as follows: ICC < 0.4 indicates poor reproducibility, 0.4 ≤ ICC < 0.75 indicates fair to good reproducibility, and ICC ≥ 0.75 indicates excellent reproducibility [64] As shown in Table 4.4 all measurements have an ICC value > 0.75 which indicates excellent agreement between the results generated by the observers. These results suggest that there is high concordance across users in the annotation of fiducial points and index lines when using the GUI.

Table 4.4: Intra-class correlation coefficient values for different measurements including SN-N distance, SN-LVP distance, and X-ratio and Y-ratio

Measurements	**SN-N**	**SN-LVP**	**X-Ratio**	**Y-Ratio**
ICC Value	0.9419	0.9291	0.8391	0.7919

Furthermore, comparison of the variability in selecting the spatial location of fiducial points was performed using the distance between the coordinates of the points selected by observer 1 and the coordinates of the same fiducial points selected by observer 2. In this study, the following criteria were used to further investigate the amount of variability in annotating the fiducial points by different users using the GUI. Tolerance thresholds were used in the classification of precision for marking points [65]. If the average distance (Davg) between two points met the condition $0 \leq \text{Davg} \leq 7$ mm, the variability between the two points was low (negligible), whereas if Davg > 7 mm, the variability in the annotation of the points was determined to be high. This criterion was based on anthropometric measurements of the diameter of the nipple, which is estimated to be in the range of 1.00–2.75 cm with a mean value of 1.53 (± 0.37) cm [63 - 67]. As a result, the criterion of $0 \leq \text{Davg} \leq 7$ mm (~radius of the nipple) was used as the criterion for low variability among the users. Also, this range is small enough to indicate the low variability in annotating other fiducial points such as sternal notch and lowest visible point as they are more subtle landmarks that are more difficult to locate.

Table 4.5 presents the result of inter-observer variability in selecting three fiducial points. In this part of the study, the distance between the nipple, sternal notch and lowest visible point marked by observer 1 and observer 2 was calculated.

Table 4.5: Inter-observer variability values for different annotated fiducial points including nipple, sternal notch and lowest visible point.

Fiducial Points	**Nipple**	**Sternal Notch**	**Lowest Visible Point**
Average Distance (mm)	3.35 ± 2.21	13.13 ± 7.79	25.54 ± 12.95

The lowest inter-observer variability was found to be in the annotation of the nipples as excepted. The average distance between the spatial location of the nipple annotated by two observers was 3.35 ± 2.21 mm which falls within the acceptable range. Whereas, in selecting sternal notch and lowest visible point, higher variability was detected as expected. The typical width of the sternal notch is about 40 mm. Due to the larger area of the sternal notch, higher variability is expected in its manual annotation, which accounts for the larger difference observed between the sternal notch annotation versus the nipple annotation across observers [67]. The location of the lateral point is ambiguous compared to the nipple and sternal notch which results in highest variability.

4.1.4 Validation of Pre-operative Nipple Position Estimates

In order to validate the multivariate linear correlation equation, a test set of pre-operative images from 20 patients (40 breasts) comprising of 5 patients from each ptosis grade (0 – 3) was utilized. The Y-ratio of these 40 breasts was calculated using the Equation 4.1 and compared to the Y-ratio for the native breast that was annotated using the GUI.

Equation 4.1: Y-ratio = -12.8*p0 – 7.6*p1 – 3.6*p2 + 0.05 * SN-N+ 64.7, where p0-p2 represents the ptosis grades 0-2.

Based on the ptosis grade of each sample, the variable corresponding to the sample's ptosis grade will be 1 and the other ptosis variables will be 0. Also, the SN-N represents the distance between sternal notch to nipple for each sample. The result is shown in Figure 4.5.

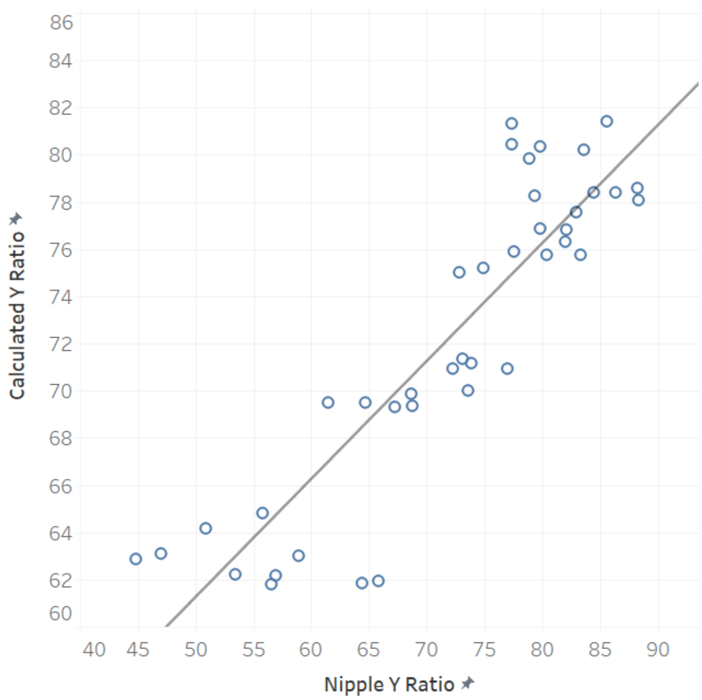

Figure 4.5: Calculated Y-ratio based on the multivariate regression vs. measured Y-ratio using GUI.

P-value<0.0001

R-Squared = 0.8

Pearson-Correlation = 0.89

This analysis indicates high correlation of the calculated Y-ratio compared to the nipple Y-ratio. As a result, Equation 4.1 can be further used to estimate the nipple Y-ratio based on the ptosis grade and the sternal notch to nipple distance.

Furthermore, in order to further investigate the estimated nipple position based on the verified multivariate linear regression, the nipple position was estimated and compared to the actual nipple position as the ground truth. In other words, the linear regressor was used to estimate the Y-ratio based on the ptosis grade and SN-N and the Y-coordinate of the nipple was then calculated based on the predicted Y-ratio. Also, as it was shown in the statistical analysis, there was no linear regression model defining the X-ratio in terms of other independent variables. As a result, the average value of the X-ratio based on all the pre-operative images was used to estimate the X-coordinate of nipple. Consequently, we compared the distance between the estimated nipple position and the actual nipple position as shown in Table 4.6. This result indicates that the linear regressor correctly predicted the Y-ratio as per p-value.

Table 4.6: Average distance between nipple position and two estimated nipple positions based on linear regressor and average ratio.

Type	**Estimated Nipple (Linear Regressor) vs Nipple**	**Estimated Nipple (Average Ratio) vs Nipple**	**P-value Paired Student's t-test $\alpha = 0.05$**
AVG Distance	14.4 ± 7.9	31.1 ± 16	4.33×10^{-8}

4.1.5. Correlation Between SN-N and SN-LVP

Univariate analysis for the pre-operative training dataset of 87 samples confirmed strong correlation across the SN-N and SN-LVP distance as shown in

A comparison of the Y-ratio computed using the multivariate model from Equation 4.1 with SN-N and the SN-LVP replaced for the SN-N was performed for the training dataset of 87 pre-operative patients indicated strong correlation (Figure 4.6). This result suggests that the multivariate model in Equation 4.1 can be used with the SN-N or SN-LVP distance.

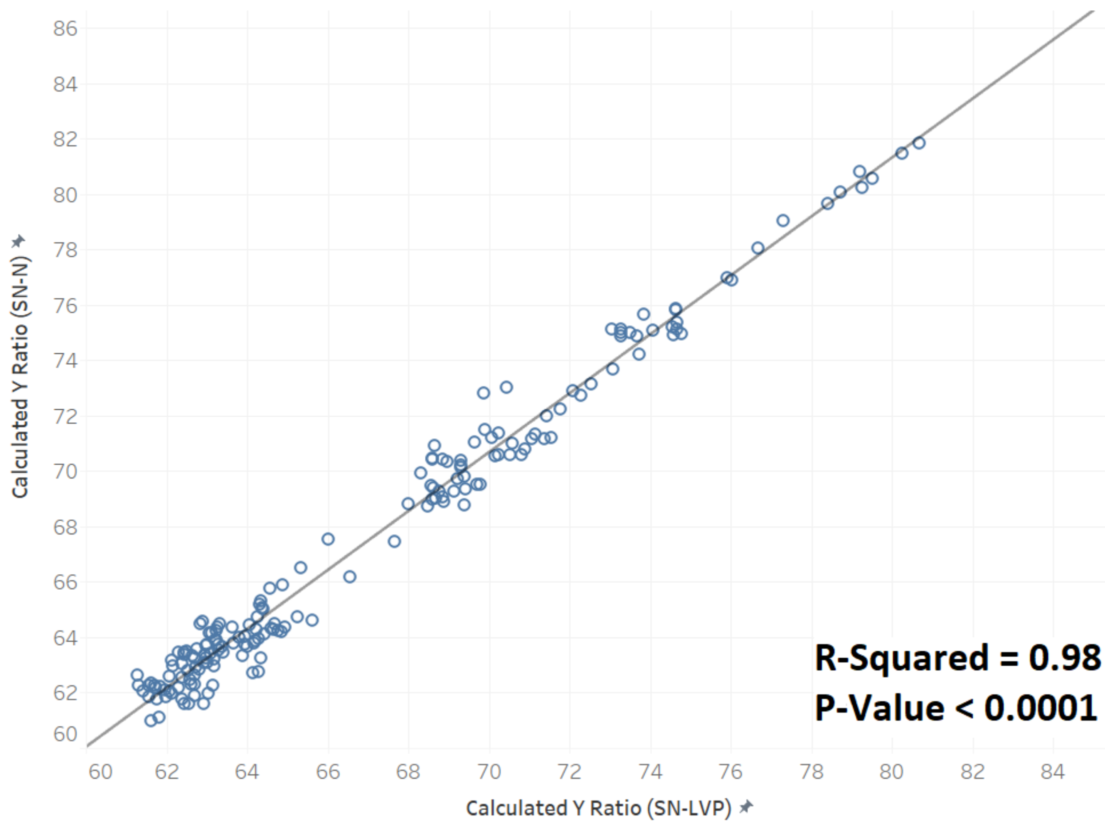

Figure 4.6: Scatter plot of calculated Y-ratio using SN-N vs calculated Y-ratio using SN-LVP.

4.1.6 Validation of Post-operative Nipple Position Estimates

Comparison of four different estimates of the nipple positions was performed using post-operative data. The nipple position based on the average ratios computed from the training set of post-operative images from 24 patients who had completed the surgery with nipple reconstruction was compared with nipple position estimates based on the following ratios reported in the literature; 40:60 X- and 40:60 Y-ratios, 40:60 X- and 50:50 Y-ratios and 50:50 X- and 50:50 Y-ratios. Two datasets were used for validation and testing. First, a set of 24 patient images at 3M time point who had TE placement and second, 14 patients at >9M time points from their baseline visit. Both datasets indicate a post-operative stage in the breast reconstruction surgery process. The location of the nipple was compared by computing the distance across the coordinates of each of the four estimated nipple positions and the ground truth nipple positions. The coordinates of the nipples annotated by a surgeon (Dr. Reece) with over 25 years of experience at the MD Anderson Cancer Center was used as the ground truth.

Table 4.7: Average distance between different suggested nipple positions and the ground truth (GT: surgeon annotated nipples) on the TE-3M dataset

Type	**Ratio based on post-operative training set**	**4060x - 5050y**	**4060x - 4060y**	**5050x - 5050y**
Distance (mm)	12.6 ± 6.6	13.5 ± 6.5	12.7 ± 5.79	22.9 ± 7.3

Table 4.7 presents the average distances between the ground truth and estimated nipple positions. The estimate based on the average ratio of the post-operative training dataset is lower than the other 3 values. Results of paired two sample Student's t-test are shown

in Table 4.8. Based on the p-values we fail to reject the null hypothesis for the ratio proposed from this study and the 4060x - 5050y and 4060x - 4060y proportions.

Table 4.8: Paired two sample t-test on distance from the actual nipple and different estimated nipples for the TE-3M dataset

	4060x - 5050y	**4060x - 4060y**	**5050x - 5050y**
Ratio based on post-operative training set	0.6	0.9	1.42×10^{-6}

In order to further investigate the best prediction for the nipple position, the same linear regressor which was validated in section 4.1.4 was used to estimate the Y-ratio of the nipple post-operatively. All the breasts in this dataset i.e., the breasts with a TE in place, were observed to have ptosis 0. So, in order to run the linear regression Equation 4.1, a value of 1 was used for p0, whereas for p1 and p2 the value was 0. Since the nipple is missing at the intermediate 3M time point, the SN-LVP distance was used instead of SN-N. The calculated Y-ratio was then used to estimate the Y-coordinate of the nipple. In addition, another estimation of Y-ratio was also calculated based on the average Y-ratio of the post-operative breasts. The average X-ratio of the post-operative breasts was used to calculate the X-coordinate of the nipple. After calculating X- and Y-coordinates of the two different estimations for nipple, the average distance between these two estimates and the ground truth was computed Table 4.9 shows the average distance between the ground truth and the two estimated nipple positions.

Table 4.9: Average distance between ground truth nipple and estimated nipples using the TE-3M dataset.

Type	Ratio from pre-operative multivariate model	Ratio based on post-operative training data	Student's t-test Paired Two Sample $\alpha = 0.05$
Distance (mm)	13.9 ± 7.8	11.6 ± 5.8	0.0003

As shown in Table 4.9, the average distance between the ground truth nipple and the estimated nipple using linear regressor is higher than the distance between the ground truth nipple and the estimated nipple using only the average ratios of the post-operative breasts. Also, a paired two samples t-test was run to further analyze the differences between these two groups of estimated nipples. The p-value of this t-test was calculated as 3.2E-5 which clearly indicates that these two measurements are significantly different. This suggests that the multivariate model for pre-operative breasts is not applicable to post-operative data at the 3M TE time point. Table 4.10 shows the results for the second data set consisting of 14 patients at >9M time points.

Table 4.10: Average distance between different suggested nipple positions and surgeon annotated nipples on post-operative dataset.

Type	Ratio based on post-operative training set	4060x - 5050y	4060x - 4060y	5050x -5050y
Distance (mm)	16 ± 9.7	18.4 ± 10.16	16 ± 8.2	26.7 ± 8.5

Moreover, in order to compare the estimated nipple based on the average post-operative ratios versus the other estimations, a paired t-test was run on this dataset as well. The result is shown in Table 4.11.

Table 4.11: Paired two samples t-test comparing the avg distance between the annotated nipple and each estimated nipple.

	4060x - 5050y	**4060x - 4060y**	**5050x - 5050y**
Ratio based on post-operative training set	0.5	0.96	0.02

The estimate based on the average ratio of the post-operative training dataset and the 40:60x and 40:60y ratio are the lowest. Results of paired two sample Student's t-test are shown in Table 4.11. Based on the p-values we fail to reject the null hypothesis for the ratio proposed from this study and the 4060x - 5050y and 4060x - 4060y proportions. Also, the linear regression Equation 4.1 was used to calculate another estimation of Y-ratio with using SN-LVP instead of SN-N and each breast's ptosis accordingly. Then, the Y-coordinate of the estimated nipples was computed using Y-ratio and the X-coordinates were also computed using the average X-ratio. Then, the distance between the annotated nipple and the estimated nipple using the linear regression (with SN-LVP instead of SN-N) for the Y-ratio and average X-ratio and also the distance between the annotated nipple and the estimated nipple using only the post-operative ratios were calculated. The result is shown in Table 4.12.

Table 4.12: Average distance of the ground truth nipple and estimated nipples using the post-operative dataset.

Type	Ratio from pre-operative multivariate model	Ratio based on post-operative training data	Student's t-test Paired Two Sample $\alpha = 0.05$
Distance (mm)	17.2 ± 9.11	16 ± 9.7	0.01

As shown in Table 4.12, the average distance between the surgeon annotated nipple and the estimated nipple using the average ratios is less than the distance between the surgeon annotated nipple and the estimated nipple based on the linear regressor using SN-LVP instead of SN-N and each ptosis grade respectively. This result indicates that, as the linear regression analyses were based on the pre-operative dataset, it is not generalizable for the post-operative breasts. In the next section, this will be further analyzed by comparing the distribution of the native breasts versus the reconstructed breasts.

An important point which needs to be mentioned here is, as the diameter of the nipple-areola complex (NAC) is estimated to be less than 2.75 cm [63, 64] any distance lower that 2.75 cm will fall within the NAC and would be clinically acceptable.

4.1.7 Nipple Position Estimate for Type of Reconstruction (Specific Objective 2)

As mentioned before, two of the most common breast reconstructions following the mastectomy are implant-based reconstruction and autologous reconstruction. The group of post-operative patients were divided to four groups based on the reconstruction type or if the breasts were intact, i.e. native breast. The result is shown in Table 4.13.

Table 4.13: Average nipple X- and Y-ratio based on the reconstruction type.

	Implant	Autologous	Native	Native with revision
Average Y-ratio	58 ± 8.1	61 ± 4.4	68 ± 6.1	58 ± 7
Average X-ratio	33 ± 6	33 ± 5.8	35 ± 5.1	34.4 ± 6
Number (%)	31 (49.2)	12 (19)	6 (9.5)	14 (22.3)

As shown in the Table 4.13, the average Y-ratio of the reconstructed breast, i.e. implant based reconstructed and autologous reconstructed and the revised native breast is less than the Y-ratio of the native breast. In order to further investigate this difference, a two sample with unequal variance t-test was run on each pair of the samples. As shown in Table 4.13, the native breast Y-ratio is significantly different when compared to all other groups. However, as all the P-values in Table 4.15 are bigger than α which is 0.05, it can be concluded that there is not any significant different in distribution of X-ratios among the post-operative breasts in terms of the reconstruction types.

Table 4.14: Two samples t-test on the Y-ratio based on the reconstruction type.

	Implant	Autologous	Native	Native with revision
Implant		0.2	0.04	0.75
Autologous	0.2		0.05	0.18
Native	0.04	0.05		0.03
Native with revision	0.75	0.18	0.03	

Table 4.15: Two samples t-test on the X-ratio based on the reconstruction type.

	Implant	Autologous	Native	Native with revision
Implant		0.93	0.63	0.63
Autologous	0.93		0.71	0.77
Native	0.63	0.71		0.89
Native with revision	0.63	0.77	0.89	

In order to better visualize the difference in data distribution based on each reconstruction type, a box plot for each reconstruction type was plotted as shown in Figure 4.7 and Figure 4.8 for X-ratio and Y-ratio respectively. This plot also shows that the native breasts have different Y-ratio distribution in compare to the breasts that underwent surgery. However, as shown in Table 4.15, there is not any significant difference in X-ratio between breasts with different reconstruction process and native breasts. This further confirms that the regression analyses which were performed on the pre-operative data cannot be used on the post-operative dataset to compute Y-ratio.

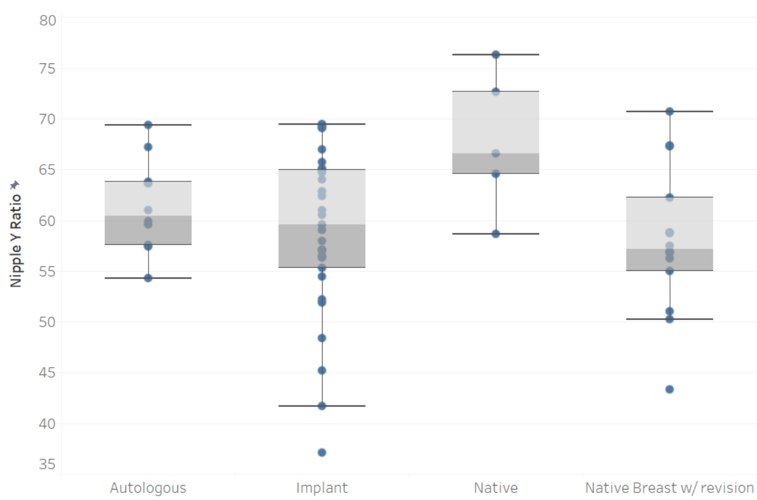

Figure 4.7: Box plot of Y-ratio for the post-operative dataset.

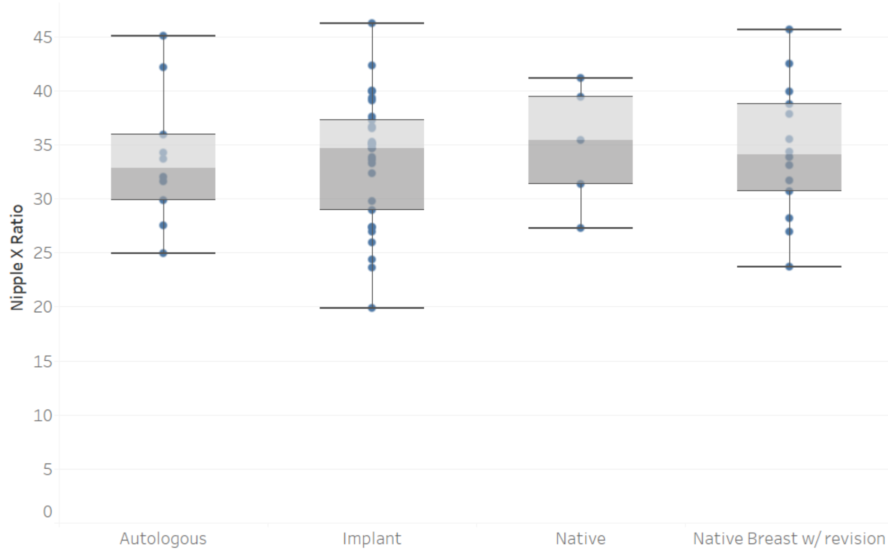

Figure 4.8: Box plot of X-ratio for the post-operative dataset.

4.1.8 Visualization of Best and Worst Estimated Nipples

As seen in the previous sections, the data driven estimates for X-ratio and Y-ratio can improve the prediction of the nipple position in pre- and post-operative data. In order to better visualize the differences, the best and worst nipple position predications for representative pre-operative and post-operative patients are presented. The red point indicates the actual nipple for the pre-operative breasts and surgeon annotated nipple position for the post-operative breasts respectively. The yellow point indicates the predicted nipple points based on the data driven proportions for X-ratio and Y-ratio determined in this study.

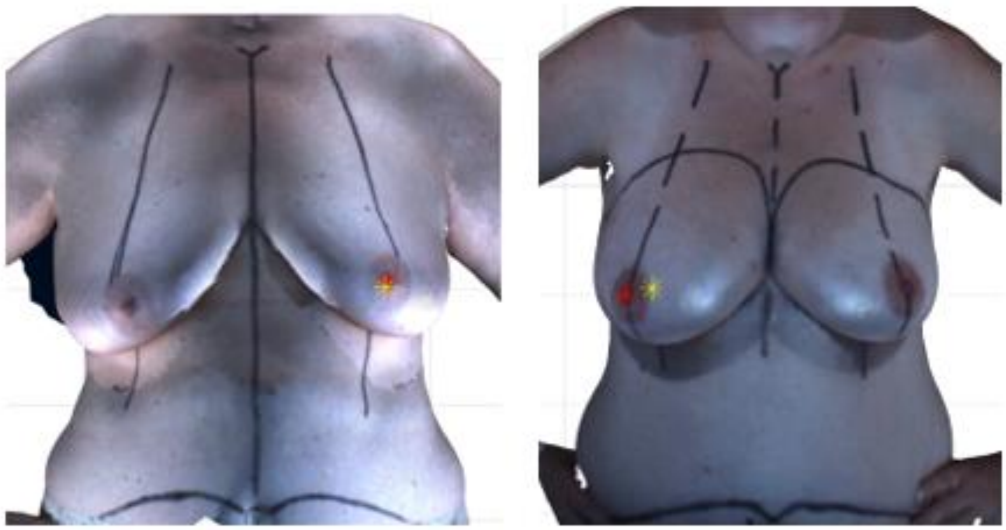

Figure 4.9: Visualization of the best (left) and the worst (right) nipple estimates for the pre-operative images. Red is the actual nipple and yellow is the predicted nipple.

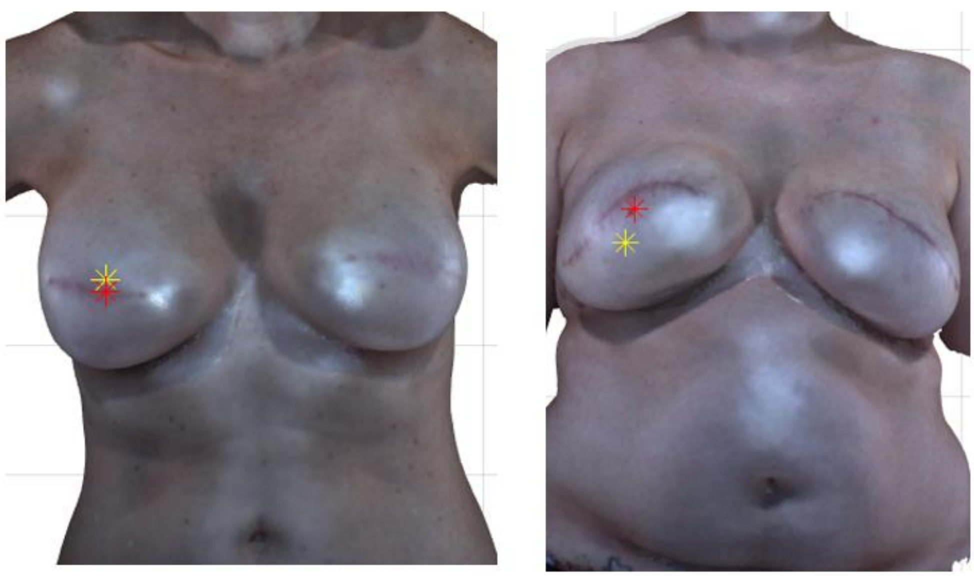

Figure 4.10: Visualization of the best (left) and the worst (right) nipple estimates for the post-operative images. Red is the surgeon annotated nipple and yellow is the predicted nipple.

4.2 Characterization of Breast Volume Measurement

In addition to determining the ratios for nipple position, experiments were conducted to characterize breast volume measurement.

4.2.1 Phantom for Breast Volume Measurements (Specific Objective 3 and 4)

In order to simulate the female torso, a flat chested mannequin (Figure 4.11 (A)) and a body suit (HPFY Medical Supplies) (Figure 4.11 (B)) were used to place a medium size adjustable implants (volume range of 550 - 660 cc) on the mannequin. 3D surface images of the mannequin were obtained using the Go!3D Scan hand-held Scanner and the 3dMDtorso system at the MD Anderson Cancer Center, Houston, TX. A set of 3D stickers were overlaid on the fiducial points marked by one of the surgeons to easily locate them on the point cloud or the 3D mesh (Figure 4.12). Breast volume for the phantom was computed using BR software as discussed earlier (Figure 4.13). As shown in Figure 4.14, volume measurement on images from the hand-held scanner is highly correlated with the volume measurements on images taken by the 3dMDtorso system.

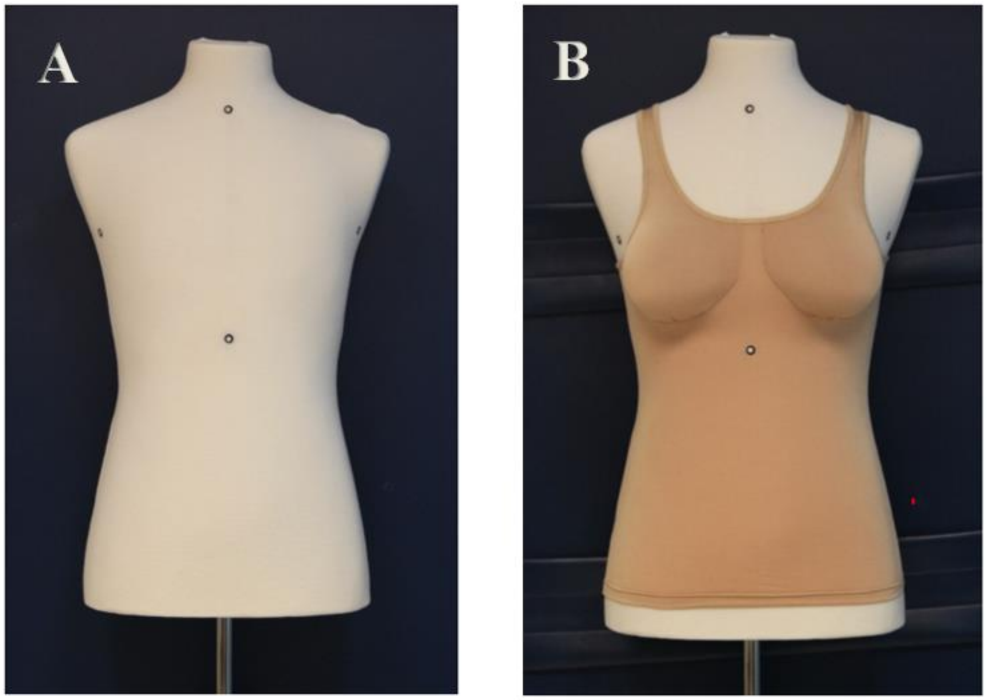

Figure 4.11: Phantom for volume measurements. (A) Flat chested mannequin and (B). Flat chested mannequin with implant inserts in the bodysuit.

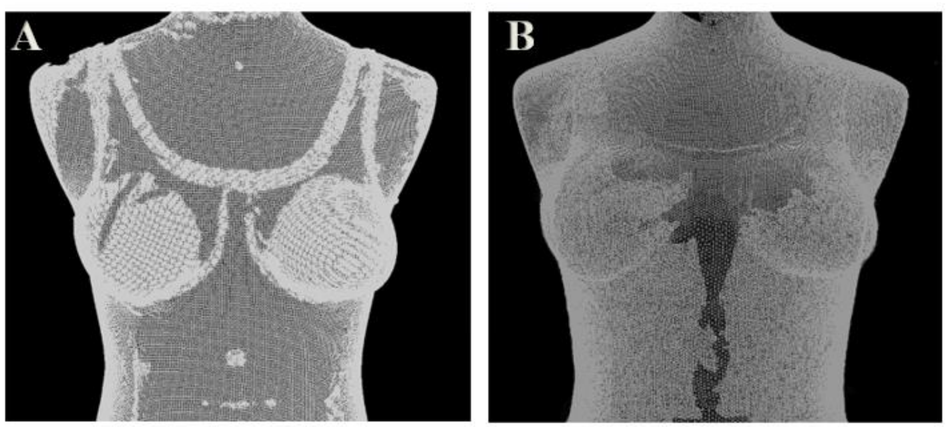

Figure 4.12: 3D mesh surface of the flat-chested mannequin with the implants using (A) hand-held scanner and (B) 3dMDtorso system.

The volume of the flatchested mannequin with the body suit but without the implants was measured and substracted from the volume measured to account for the material of the bodysuit. In addition, the volume of the empty implant was measured as well in order to take into account the volume of the empty implant.

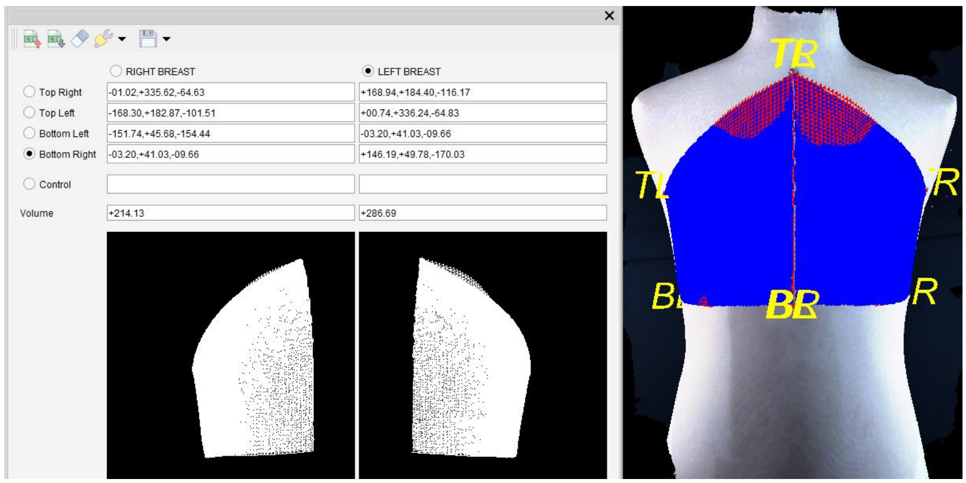

Figure 4.13:Volume measurement of the flat-chested mannequin.

The volume of the empty implant was estimated from its weight and density as shown in Equation 4.2.

Empty Implant Weight = 46 gr.

Implant Density = 0.975 gr/cc.

Empty Implant Volume= 46/0.975 = 47.18 cc

Equation 4.2: Volume measurement for empty implant.

The final volume measured was adjusted by subtracting the value of mannequin chest (bodysuit material) and the volume of the empty implant.

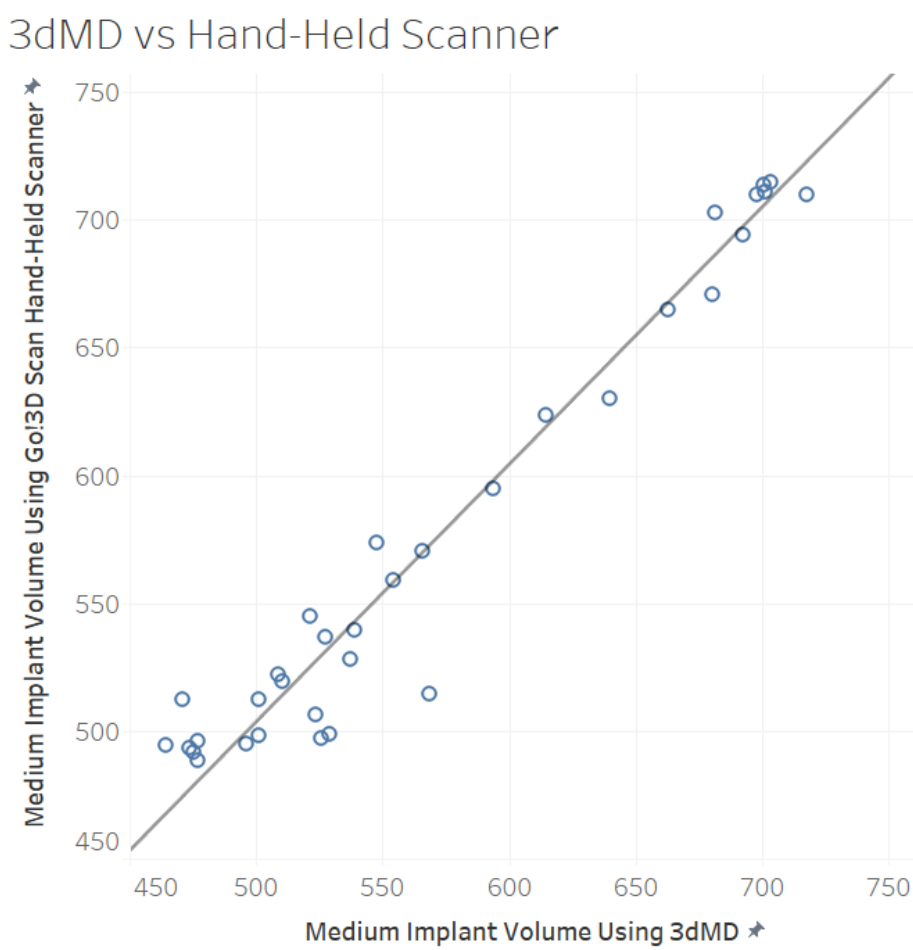

Figure 4.14: Scatter plot of the measured volume of the images taken by the hand-held scanner vs the measured volume of the images taken by 3dMD system.

The equation of the trend line shown in the Figure 4.14 is as follows:

Measured Volume using Go!3D Scan Hand-Held Scanner: V_{HH}

Measured Volume using 3dMDtorso™ system: V_{3dMD}

$$V_{HH} = 1.007 * V_{3dMD}$$

Equation 4.3: The regressor line equation of the measured volume of the image taken by hand-held scanner in terms of the measured volume of the image taken by 3dMD system.

The calculated R-Squared value is 0.999 and the p-value is less than 0.001 which shows that the volume calculated using 3dMD imaging system is highly correlated with the volume calculated using handheld scanner. This verifies the ability of the 3D handheld scanner in capturing 3D surface images that enable quantitative measurements of volume similar to that of expensive stereophotography systems. In addition, using the hand-held scanner gives the clinicians the ability to scan the patient's torso through 360°, while using the 3D stereophotogrammetry systems do have this feature and it only can capture the frontal surface through 180°.

4.2.2 Investigation of the Smallest Measurable Volume (Specific Objective 5)

In this part of the study, the adjustable volume breast implants were used and fitted with a fill tube for allowing injection of varying amounts of water to achieve desired size adjustments. Three different sizes of adjustable implants (354-2511: 275–330 cc, 354-2514: 550–660 cc, and 354-2515: 650–780 cc) were donated by Mentor Worldwide LLC, Irvine, CA. The implants were painted with washable paints to minimize reflective glare and 3D surface images were acquired using the 3dMDtorso™ system (3dMD® LLC, Atlanta, GA). Each volume measurement was performed 3 times and averaged to mitigate the random error which might happen during the volume measurement process. As shown in Figure 4.15, the volume of the implant was measured using BR software. In addition, Figure 4.16 presents a plot of the measured volume versus the injected volume. To determine the smallest volume detectable, the volume difference was computed across each sequential image (5 cc change) and across every second sequential image (10 cc change) and was measured to be 5.51 ± 2.95 cc and 10.86 ± 3.36 cc, respectively.

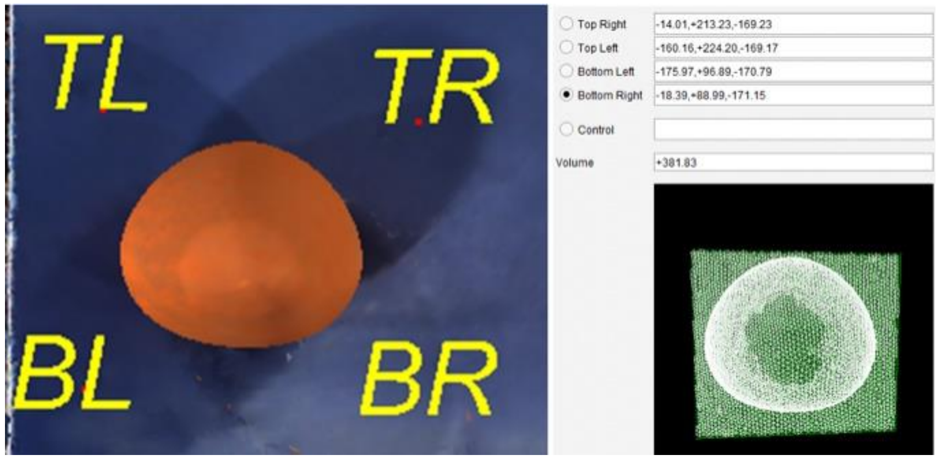

Figure 4.15: Volume was measured as that enclosed between the implant surface and the coons patch bound by points; TL: top left, TR: top right, BR; bottom right, and BL: bottom left.

In order to account for the volume of the empty (unfilled) implant, the empty implant volume was calculated using its weight and density as shown in Equation 4.4. The amount of measured volume adjusted by subtracting the volume of the empty implant. As seen in Figure 4.16, there is a linear correspondence between the measured volume and the injected volume ($R^2 > 0.99$). This data suggests that 3D imaging can successfully measure volume and can reliably detect changes in volume as low as 5 cc for implants of varying sizes.

Empty Small Implant Weight = 31.6 gr.

Implant Density = 0.975 gr/cc.

Empty Small Implant Volume = 31.6/0.975 = 32.41 cc

Empty Medium Implant Weight = 46 gr.

Implant Density = 0.975 gr/cc.

Empty Small Implant Volume = 46/0.975 = 47.18 cc

Empty Large Implant Weight = 53.2 gr.

Implant Density = 0.975 gr/cc.

Empty Small Implant Volume= 53.2/0.975 = 54.56 cc

Equation 4.4: Volume calculation for the 3 different implants when empty.

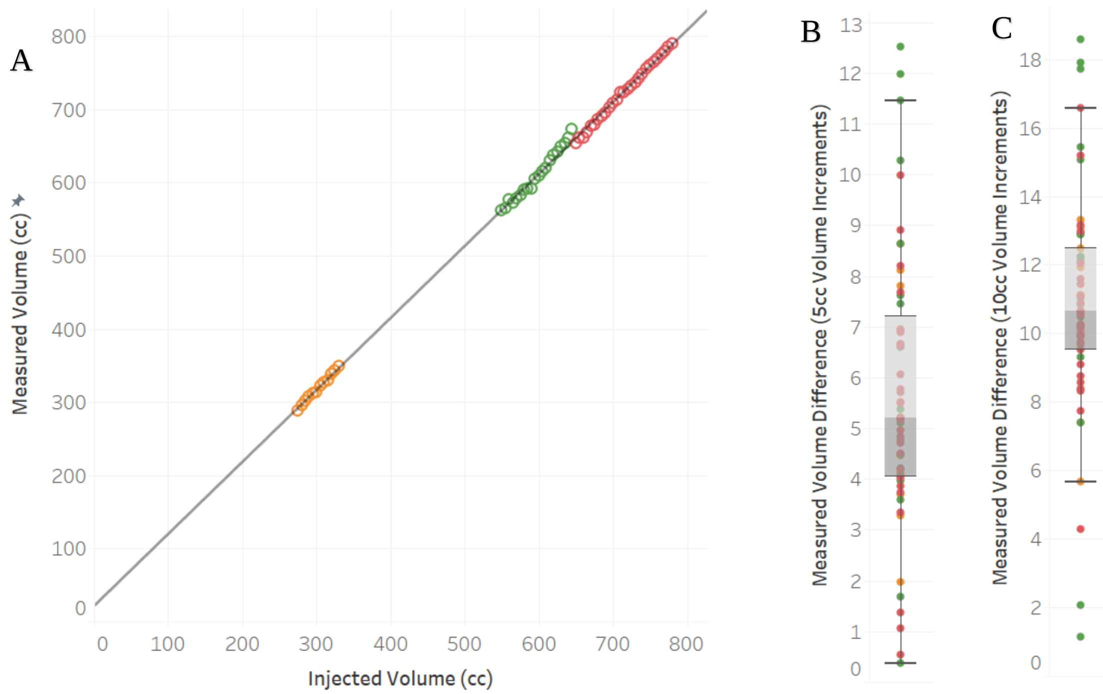

Figure 4.16: Volume measurements in adjustable implants. (A) Measured volume versus injected volume, (B-C) Box plot of measured volume difference across incremental volume steps of 5 cc and 10 cc.

The equation of the line depicted in above figure is as follows:

Measured Volume = V_m Injected Volume = V_i

$V_m = 1.016 * V_i$ R-squared = 0.9998 P-value < 0.0001 Equation 4.5

Table 4.16: P-value of the Students t-test for two sample equal variance.

Students T-Test
Two sample equal variance
Two tail, α=0.05
(5 vs. 10 cc volume difference)

Implant Size (cc)	P-value
275 – 330	6.5×10^{-5}
550 – 660	5.1×10^{-4}
650 – 780	2.9×10^{-10}

This shows an almost perfect collinearity which indicates the ability to detect small volume changes while maintaining high accuracy.

CHAPTER 5 CONCLUSIONS AND DISCUSSION

In this study, I have demonstrated different quantified metrics which not only are important in assessing the result of breast reconstruction surgery, but also are essential in facilitating the patient-surgeon clinical communication in shared decision-making process. In this regard, we have analyzed two important approaches. First, locating the position of the nipple and second measuring the smallest breast volume changes while maintaining the highest possible accuracy.

However, by doing this study, I aimed to convey a more significant message which I found absent in many of the published papers. As mentioned in the related works section, many researchers conducted studies by showing the model images with using a term such as perfect, ideal, more sexual or best nipple position/breast shape and further asked the observers to rank them in order to come up with some golden metrics in defining these breasts shapes/nipple positions. A point which is worth mentioning here is, however we can utilize these metrics in post-operative planning, i.e. after mastectomy surgery, women population comprises of different humans with different breast sizes, breast shapes, nipple positions, skin colors, nipple pigmentation colors, races, ethnicities etc. I aimed to show that there is not a single ground truth metric which can be utilized for all the patients and none of the mentioned metrics is superior on others in terms of indicating the “idealness” of the breast shape or nipple position. Therefore, in order to address this limitation in the published literatures, a dataset including images of the natural breasts from different demographic distributions was used. In addition, multiple statistical analyses were used to better present this diversity among the women and their body characteristics.

Furthermore, in order to help the patients who have already gone through the mastectomy surgery, using the available literatures, I developed a graphical user interface with the ability to determine and visualize some personalized nipple positions for the reconstructed breasts. As a result, this will facilitate physician-patient communication during clinical consultations. The GUI in conjunction with the multiple regression model will allow visualizations of personalized nipple positions for patients.

Furthermore, I have proposed a method to create a mannequin-based phantom to simulate the female torso, with the ability to manipulate breast volume in customizable increments/decrements. The phantom can be utilized to assess the resolution of 3D imaging for volume measurements as well as to investigate the applicability of using a 3D hand-held scanner in the clinics. Using the adjustable implants, the smallest measurable volume changes was measured which can help in estimating retention of fat grafts that are frequently used for contour shaping in reconstructive breast surgery. This will help the caregivers in assessing the volume changes over time as well as in analyzing the volume symmetry between both breasts.

In summary, this research achieved the following;

1. Developed a GUI for quantifying nipple position
2. Developed an algorithm for estimation of nipple position in pre-operative breasts
3. Presented normative data on association of nipple position with breast shape
4. Developed a phantom to better simulate different breast sizes.
5. Established usability of portable hand-held scanner.

6. Determined the minimum volume measurable by 3D imaging for evaluating volume changes.
7. This research has potential to assist physicians in surgical planning and improve physician-patient communication during clinical consultation.

CHAPTER 6 FUTURE WORK

In the future work, we will work on incorporating more data to our model for running the regression analyses on the post operation data as well. Furthermore, we are planning to add more data of the post-operative images with different type of the reconstruction surgeries to evaluate the suggested nipple positions based on the type of reconstructions. Using this dataset will enable us to investigate different nipple ratios suitable for each type of reconstruction surgery, such as autologous or implant-based reconstruction. This will offer personalized predictions which will help both patient and surgeon in operation planning and will improve the quality of care. This will also result in decreasing the need for follow up surgeries which help the patient to retain her physical and psychosocial well-being.

In addition, we will add the visualization of the estimated nipple position using the regression models, for both pre-operative and post-operative images to the GUI. So, that the user can enter the required values for the regression model and can see the result based on the entered values.

Regarding the second part of the study in which we analyzed the smallest measurable volume, future work will focus on determining the smallest volume perceptible qualitatively by human observers.

REFERENCES

[1] Torre, L. A., Bray, F., Siegel, R. L., Ferlay, J., Lortet-Tieulent, J., & Jemal, A. (2015). Global cancer statistics, 2012. *CA: A Cancer Journal for Clinicians*, *65*(2), 87–108.

[2] "U.S. Breast Cancer Statistics." [Online]. Available: https://www.breastcancer.org/symptoms/understand_bc/statistics [Accessed: 22-June-2020].

[3] "Survival Rates for Breast Cancer "[Online]. Available: 22-June-2020].

[4] Enajat, M., Smit, J. M., Rozen, W. M., Hartman, E. H., Liss, A., Kildal, M., ... & Acosta, R. (2010). Aesthetic refinements and reoperative procedures following 370 consecutive DIEP and SIEA flap breast reconstructions: important considerations for patient consent. *Aesthetic plastic surgery*, *34*(3), 306-312.

[5] Wilting, F. N., Hameeteman, M., Tielemans, H. J., Ulrich, D. J., & Hummelink, S. (2020). Three-dimensional evaluation of breast volume changes following autologous free flap breast reconstruction over six months. *The Breast*, *50*, 85-94.

[6] Lee, Woo Yeon, et al. "Three-dimensional surface imaging is an effective tool for measuring breast volume: a validation study." *Archives of plastic surgery* 43.5 (2016): 430.

[7] "BREAST RECONSTRUCTION" [Online] Available: [Accessed: 07-01-2020]

[8] "TRAM Flap." [Online]. Available: http://www.breastreconstruction.org/TypesOfReconstruction/tram_flap.html [Accessed: 22-June-2020].

[9] "Direct to Implant ("One-Step") Breast Reconstruction." [Online]. Available: http://www.breastreconstruction.org/TypesOfReconstruction/direct_to_implant.html [Accessed: 22-June-2020].

[10] Dikmans, R. E., Nene, L. E., Bouman, M. B., de Vet, H. C., Mureau, M. A., Buncamper, M. E., ... & Mullender, M. G. (2017). The aesthetic items scale: a tool for the evaluation of aesthetic outcome after breast reconstruction. *Plastic and Reconstructive Surgery Global Open*, *5*(3).

[11] Tevis, S. E., James, T. A., Kuerer, H. M., Pusic, A. L., Yao, K. A., Merlino, J., & Dietz, J. (2018). Patient-reported outcomes for breast cancer. *Annals of surgical oncology*, *25*(10), 2839-2845.

[12] Karatas, O. H., & Toy, E. (2014). Three-dimensional imaging techniques: A literature review. *European journal of dentistry*, *8*(01), 132-140.

[13] R. L. O'Connell, R. J. G. Stevens, P. A. Harris, and J. E. Rusby, "Review of three-dimensional (3D) surface imaging for oncoplastic, reconstructive and aesthetic breast surgery," *Breast*, vol. 24, no. 4, pp. 331–342, 2015.

[14] Joda, T., & Gallucci, G. O. (2015). The virtual patient in dental medicine. *Clinical oral implants research*, *26*(6), 725-726.

[15] Yee, A., Harmon, J., & Yi, S. (2016). Quantitative monitoring wound healing status through three-dimensional imaging on mobile platforms. *Journal of the American College of Clinical Wound Specialists*, *8*(1-3), 21-27.

[16] Hsu, P. J., Denadai, R., Pai, B. C., Lin, H. H., & Lo, L. J. (2020). outcome of facial contour asymmetry after conventional two-dimensional versus computer-assisted three-dimensional planning in cleft orthognathic surgery. *Scientific Reports*, *10*(1), 1-12.

[17] R. Zheng, W. Yu, and J. Fan, "Development of a new chinese bra sizing system based on breast anthropometric measurements," *Int. J. Ind. Ergon.*, vol. 37, no. 8, pp. 697–705, 2007.

[18] D. K. Avşar, A. C. Aygit, E. Benlier, H. Top, and O. Taşkinalp, "Anthropometric breast measurement: a study of 385 Turkish female students.," *Aesthet. Surg. J.*, vol. 30, no. 1, pp. 44–50, 2010.

[19] P. Agbenorku, M. Agbenorku, A. Iddi, E. Amevor, R. Sefenu, and D. Osei, "Measurements of breasts of young West African females: a guideline in anatomical landmarks for adolescent breast surgery.," *Aesthetic Plast. Surg.*, vol. 35, no. 1, pp. 49–54, 2011.

[20] Wilting, F. N., Hameeteman, M., Tielemans, H. J., Ulrich, D. J., & Hummelink, S. (2020). Three-dimensional evaluation of breast volume changes following autologous free flap breast reconstruction over six months. *The Breast*, *50*, 85-94.

[21] Wilting FNH, Hameeteman M, Tielemans HJP, Ulrich DJO, Hummelink S. Breast. 2020 Apr;50:85-94. doi: 10.1016/j.breast.2020.02.005. Epub 2020 Feb 10. PMID: 32113147

[22] Li, D., Cheong, A., Reece, G. P., Crosby, M. A., Fingeret, M. C., & Merchant, F. A. (2016). Computation of breast ptosis from 3D surface scans of the female torso. *Computers in biology and medicine*, *78*, 18-28.

[23] Teo, I., Reece, G. P., Huang, S. C., Mahajan, K., Andon, J., Khanal, P., ... & Fingeret, M. C. (2018). Body image dissatisfaction in patients undergoing breast reconstruction: Examining the roles of breast symmetry and appearance investment. *Psycho-oncology*, *27*(3), 857-863.

[24] Cheong, A. L., Liu, J., Reece, G. P., Nicklaus, K. M., Bordes, M. C., Hanson, S. E., ... & Merchant, F. A. (2019). Natural breast symmetry in preoperative breast cancer patients. *Plastic and reconstructive surgery Global open*, *7*(7).

[25] Henseler, H., Ju, X., Ayoub, A., & Ray, A. K. (2013). The importance of the pose in three-dimensional imaging of the ptotic breast. *Journal of Plastic, Reconstructive & Aesthetic Surgery*, *66*(11), 1551-1556.

[26] Beesley, H., Ullmer, H., Holcombe, C., & Salmon, P. (2012). How patients evaluate breast reconstruction after mastectomy, and why their evaluation often differs from that of their clinicians. *Journal of plastic, reconstructive & aesthetic surgery*, *65*(8), 1064-1071.

[27] Al-Ghazal, S. K., Fallowfield, L., & Blamey, R. W. (2000). Comparison of psychological aspects and patient satisfaction following breast conserving surgery, simple mastectomy and breast reconstruction. *European journal of cancer*, *36*(15), 1938-1943.

[28] Serletti, J. M., Fosnot, J., Nelson, J. A., Disa, J. J., & Bucky, L. P. (2011). Breast reconstruction after breast cancer. *Plastic and Reconstructive Surgery*, *127*(6), 124e-135e.

[29] Teo, I., Reece, G. P., Christie, I. C., Guindani, M., Markey, M. K., Heinberg, L. J., ... & Fingeret, M. C. (2016). Body image and quality of life of breast cancer patients: influence of timing and stage of breast reconstruction. *Psycho-Oncology*, *25*(9), 1106-1112.

[30] Somogyi, R. B., Ziolkowski, N., Osman, F., Ginty, A., & Brown, M. (2018). Breast reconstruction: Updated overview for primary care physicians. *Canadian Family Physician*, *64*(6), 424-432.

[31] Cheong, A. L., Liu, J., Reece, G. P., Nicklaus, K. M., Bordes, M. C., Hanson, S. E., ... & Merchant, F. A. (2019). Natural breast symmetry in preoperative breast cancer patients. *Plastic and reconstructive surgery Global open*, *7*(7).Rinker B, Veneracion M, Walsh CP. Breast ptosis: causes and cure. *Ann Plast Surg*. 2010;64:579–84.

[32] Atiye, B., & Chahine, F. (2018). Metrics of the aesthetically perfect breast. *Aesthetic Plastic Surgery*, *42*(5), 1187-1194.

[33] Hwang, K., Park, J. Y., & Hwang, S. W. (2015). A consideration of breast imagery in art as depicted through western painting. *Archives of plastic surgery*, *42*(2), 226.

[34] Atiye, B., & Chahine, F. (2018). Metrics of the aesthetically perfect breast. *Aesthetic Plastic Surgery*, *42*(5), 1187-1194.

[35] Raposio, E., Belgrano, V., Santi, P., & Chiorri, C. (2016). Which is the ideal breast size?: Some social clues for plastic surgeons. *Annals of Plastic Surgery*, *76*(3), 340-345.

[36] Zelazniewicz, A. M., & Pawlowski, B. (2011). Female breast size attractiveness for men as a function of sociosexual orientation (restricted vs. unrestricted). *Archives of Sexual Behavior*, *40*(6), 1129-1135.

[37] Kościński, K. (2019). Breast firmness is of greater importance for women's attractiveness than breast size. *American Journal of Human Biology*, *31*(5), e23287.

[38] Martinovic, M. E., & Blanchet, N. P. (2017). BFACE: a framework for evaluating breast aesthetics. *Plastic and Reconstructive Surgery*, *140*(2), 287e-295e.

[39] Blondeel, P. N., Hijjawi, J., Depypere, H., Roche, N., & Van Landuyt, K. (2009). Shaping the breast in aesthetic and reconstructive breast surgery: an easy three-step principle. *Plastic and reconstructive surgery*, *123*(2), 455-462.

[40] Groyecka, A., Żelaźniewicz, A., Misiak, M., Karwowski, M., & Sorokowski, P. (2017). Breast shape (ptosis) as a marker of a woman's breast attractiveness and age: Evidence from Poland and Papua. *American Journal of Human Biology*, *29*(4), e22981.

[41] Bykowski, M. R., Emelife, P. I., Emelife, N. N., Chen, W., Panetta, N. J., & de la Cruz, C. (2017). Nipple–areola complex reconstruction improves psychosocial and sexual well-being in women treated for breast

cancer. *Journal of Plastic, Reconstructive & Aesthetic Surgery*, *70*(2), 209-214.

[42] Goh, S. C. J., Martin, N. A., Pandya, A. N., & Cutress, R. I. (2011). Patient satisfaction following nipple-areolar complex reconstruction and tattooing. *Journal of plastic, reconstructive & aesthetic surgery*, *64*(3), 360-363.

[43] Lewin, R., Amoroso, M., Plate, N., Trogen, C., & Selvaggi, G. (2016). The aesthetically ideal position of the nipple–areola complex on the breast. *Aesthetic Plastic Surgery*, *40*(5), 724-732.

[44] Mett, T. R., Krezdorn, N., Luketina, R., Boyce, M. K., Henseler, H., Ipaktchi, R., & Vogt, P. M. (2017). Optimal positioning of the nipple–areola complex in men using the Mohrenheim-Estimated-Tangential-Tracking-Line (METT-Line): An intuitive approach. *Aesthetic Plastic Surgery*, *41*(6), 1295-1302.

[45] Lewin, R., Widmark-Jensen, E., Plate, N., & Hansson, E. (2018). Objective evaluation of nipple position after 336 breast reductions. *Journal of Plastic Surgery and Hand Surgery*, *52*(4), 198-203.

[46] Laschuk, M. J., Head, L. K., Roumeliotis, G. A., Xuan, L., & Silverman, H. J. (2020). The rule of thirds: Determining the ideal areolar proportions. *JPRAS open*, *23*, 55-59.

[47] Pereira Filho, O., Ely, J. B., Lee, K. H., Paulo, E. M., & Granemann, A. S. (2019). Multiplanar Assembly Mammaplasty Based on the Divine Proportion. *Plastic and Reconstructive Surgery Global Open*, *7*(2).

[48] Guyomard, V., Leinster, S., & Wilkinson, M. (2007). Systematic review of studies of patients' satisfaction with breast reconstruction after mastectomy. *The Breast*, *16*(6), 547-567.

[49] Craft, R. O., Colakoglu, S., Curtis, M. S., Yueh, J. H., Lee, B. S., Tobias, A. M., & Lee, B. T. (2011). Patient satisfaction in unilateral and bilateral breast reconstruction [outcomes article]. *Plastic and reconstructive surgery*, *127*(4), 1417-1424.

[50] Henseler, H., Ju, X., Ayoub, A., & Ray, A. K. (2013). The importance of the pose in three-dimensional imaging of the ptotic breast. *Journal of Plastic, Reconstructive & Aesthetic Surgery*, *66*(11), 1551-1556.

[51] Kayar, R., Civelek, S., Cobanoglu, M., Gungor, O., Catal, H., & Emiroglu, M. (2011). Five methods of breast volume measurement: a comparative study of measurements of specimen volume in 30 mastectomy cases. *Breast cancer: basic and clinical research*, *5*, BCBCR-S6128.

[52] Smith Jr, D. J., Palin Jr, W. E., Katch, V. L., & Bennett, J. E. (1986). Breast volume and anthropomorphic measurements: normal values. *Plastic and reconstructive surgery*, *78*(3), 331-335.

[53] Rha, E. Y., Choi, I. K., & Yoo, G. (2014). Accuracy of the method for estimating breast volume on three-dimensional simulated magnetic resonance imaging scans in breast reconstruction. *Plastic and Reconstructive Surgery*, *133*(1), 14-20.

[54] Neal, A. J., Torr, M., Helyer, S., & Yarnold, J. R. (1995). Correlation of breast dose heterogeneity with breast size using 3D CT planning and dose-volume histograms. *Radiotherapy and oncology*, *34*(3), 210-218.

[55] Malini, S., Smith, E. O. B., & Goldzieher, J. W. (1985). Measurement of breast volume by ultrasound during normal menstrual cycles and with oral contraceptive use. *Obstetrics & Gynecology, 66*(4), 538-541.

[56] Gorczyca, D. P., Gorczyca, S. M., & Gorczyca, K. L. (2007). The diagnosis of silicone breast implant rupture. *Plastic and reconstructive surgery*, *120*(7), 49S-61S.

[57] O'Connell, R. L., Khabra, K., Bamber, J. C., deSouza, N., Meybodi, F., Barry, P. A., & Rusby, J. E. (2018). Validation of the Vectra XT three-dimensional imaging system for measuring breast volume and symmetry following oncological reconstruction. *Breast Cancer Research and Treatment*, *171*(2), 391-398.

[58] Wesselius, T. S., Verhulst, A. C., Vreeken, R. D., Xi, T., Maal, T. J., & Ulrich, D. J. (2018). Accuracy of three software applications for breast volume calculations from three-dimensional surface images. *Plastic and reconstructive surgery*, *142*(4), 858-865.

[59] Okoli, C., & Pawlowski, S. D. (2004). The Delphi method as a research tool: an example, design considerations and applications. Information & management, 42(1), 15-29. McGraw, K. O., & Wong, S. P. (1996). Forming inferences about some intraclass correlation coefficients. *Psychological methods*, *1*(1), 30.

[60] Goyal, A. (2015). The development of a low cost 3D surface imaging system to measure breast volume: Defining minimum standards using an adapted Delphi consensus study.

[61] Reece, G. P., Merchant, F., Andon, J., Khatam, H., Ravi-Chandar, K., Weston, J., ... & Markey, M. K. (2015). 3D surface imaging of the human female torso in upright to supine positions. *Medical engineering & physics*, *37*(4), 375-383.

[62] "[Hands-on] Test and review of the Creaform Go!SCAN 50, a professional-grade portable 3D scanner." [Online]. Available: https://www.aniwaa.com/blog/hands-on-test-and-review-of-the-creaform-goscan-50-portable-3d-scanner/ [Accessed: 22-June-2020].

[63] Lee, J., Kawale, M., Merchant, F. A., Weston, J., Fingeret, M. C., Ladewig, D., ... & Markey, M. K. (2011). Validation of stereophotogrammetry of the human torso. *Breast cancer: basic and clinical research*, *5*, BCBCR-S6352.

[64] Kawale, M., Lee, J., Leung, S. Y., Fingeret, M. C., Reece, G. P., Crosby, M. A., ... & Merchant, F. A. (2011). 3D symmetry measure invariant to subject pose during image acquisition. *Breast cancer: basic and clinical research*, *5*, BCBCR-S7140.

[65] Kovacs, L., Zimmermann, A., Brockmann, G., Baurecht, H., Schwenzer-Zimmerer, K., Papadopulos, N. A., ... & Zeilhofer, H. F. (2006). Accuracy and precision of the three-dimensional assessment of the facial surface using a 3-D laser scanner. *IEEE transactions on medical imaging*, *25*(6), 742-754.

[66] Kawale, M. M., Reece, G. P., Crosby, M. A., Beahm, E. K., Fingeret, M. C., Markey, M. K., & Merchant, F. A. (2013). Automated identification of fiducial

points on 3D Torso images. Biomedical engineering and computational biology, 5, BECB-S11800.

[67] Avşar, D. K., Aygıt, A. C., Benlier, E., Top, H., & Taşkınalp, O. (2010). Anthropometric breast measurement: a study of 385 Turkish female students. *Aesthetic Surgery Journal*, *30*(1), 44-50.